Song *et al.*
Chinese Journal of Mechanical Engineering (2023) 36:139
https://doi.org/10.1186/s10033-023-00961-y

Chinese Journal of Mechanical Engineering

REVIEW

Open Access

Effects of Electric and Magnetic Treatments on Microstructures of Solid Metals: A Review

Yanli Song[1,2,3,4*], Wenlin Wu[3], Yongqing Yu[3] and Lin Hua[1,2,3,4]

Abstract

An external electric or magnetic field can transfer high-intensity energy directly to the electronic scale of materials, and change the spin, energy level arrangement and trajectory of electrons. These changes produce tremendous and profound impacts on the microstructure and mechanical properties of metal materials, which may be impossible with traditional technologies. This paper reviews the effects of electric or magnetic field on the microstructures of solid metals including phase transformation, precipitation, recrystallization, dislocations and so on. Based on the existing research results, the mechanisms of these effects have been discussed. Additionally, some typical applications of electric and magnetic treatments on solid metals have been described and the challenges in this field have also been discussed.

Keywords Electric field, Magnetic field, Microstructures, Mechanical properties, Solid metals

1 Introduction

Metal materials are widely used in aerospace, automobile, ships, high-speed railways and other industries due to their excellent mechanical properties. The service performance and life of products usually depend on the properties of materials, thus always attracting extensive attentions of material scientists [1, 2]. As the most popular method to improve the mechanical properties of metal materials, heat treatment, however, remain a series of drawbacks [3, 4], such as time and energy-consuming, oxidation of products, and large deformation. Therefore, it is of greatly practical significance to explore a stable, efficient and environment-friendly method to enhance the material properties.

*Correspondence:
Yanli Song
ylsong@whut.edu.cn
[1] Hubei Key Laboratory of Advanced Technology for Automotive Components, Wuhan University of Technology, Wuhan 430070, China
[2] Hubei Collaborative Innovation Center for Automotive Components Technology, Wuhan University of Technology, Wuhan 430070, China
[3] School of Automotive Engineering, Wuhan University of Technology, Wuhan 430070, China
[4] Hubei Research Center for New Energy & Intelligent Connected Vehicle, Wuhan University of Technology, Wuhan 430070, China

In recent decades, many studies have shown that electromagnetic treatment can improve the mechanical properties of metal materials. According to the form of external applied energy, electromagnetic treatment can be divided into electric field or current treatment (ET), magnetic field treatment (MT) and the combination treatment of electric and magnetic fields (ET&MT). These external fields can exert Coulomb force on a charged particle or Lorentz force on a moving charged particle to affect their migration or diffusion.

In 1963, Troitskii and Likhtman [5] reported that the elongation of Zinc single crystals was increased significantly by loading current under uniaxial tension condition. Zagoruiko [6] discovered that alternating magnetic field can affect the plasticity of NaCl crystals in 1965. Subsequently, a considerable amount of efforts have been made to investigate the effect of electric and magnetic fields on the plasticity of metal materials [7–11]. As is well known, the plasticity of nearly all metal materials in electric and magnetic fields is changed to some extent, which is so-called "electro-plasticity" or "magneto-plasticity" [12]. In addition, it was found that great progress in metal properties, in terms of the improvement in the residual stress [13–16], the

© The Author(s) 2023. **Open Access** This article is licensed under a Creative Commons Attribution 4.0 International License, which permits use, sharing, adaptation, distribution and reproduction in any medium or format, as long as you give appropriate credit to the original author(s) and the source, provide a link to the Creative Commons licence, and indicate if changes were made. The images or other third party material in this article are included in the article's Creative Commons licence, unless indicated otherwise in a credit line to the material. If material is not included in the article's Creative Commons licence and your intended use is not permitted by statutory regulation or exceeds the permitted use, you will need to obtain permission directly from the copyright holder. To view a copy of this licence, visit http://creativecommons.org/licenses/by/4.0/.

promotion of wear resistances [17–19], the extension of the fatigue life [20–22] and the modification of the resistivity [23–25], has also been obtained by an external electric or magnetic treatment.

It is well known that the properties of metal materials are determined by their internal microstructures such as crystal structures, crystal defects, phase composition, grain sizes and morphology, etc. Therefore, the desired mechanical properties can be obtained via the exquisite design of material microstructures. Regrettably, the microstructures formed by the traditional processes are usually to achieve the strength-ductility trade-off [26]. Nevertheless, a few recent efforts seem to confirm that this limitation can be conquered. Both nano-scale precipitates and high density dislocations, for instance, could improve the strength and ductility simultaneously [2, 27]. Relevant literatures reported that the aforementioned extraordinary microstructures of metal materials, which may lead to excellent material properties, are also expected to be also obtained by ET or MT [28].

After decades of exploration by scientific researchers and engineers, the applications of ET and MT in industry have gradually sprung out in recent years. These phenomena mainly derived from the profound understanding of the effects of electric and magnetic fields on the solid metals. To grasp the latest research progress and development trend, we summarized and analyzed the effects of electric and magnetic fields on the microstructures of solid metal and its potential mechanism, and attempted to explore the internal relationship of these phenomena. In addition, some challenges hindering the development of theory and application of these processes are also discussed.

2 Effects of ET on Microstructures of Solid Metals

2.1 Effects of ET on Phase Evolution

2.1.1 Effects of ET on Solid Phase Transition

A current can induce phase transformations of metals and alloys. It generally has the characteristics of faster speed, lower temperature and finer product than heat treatment. Chu et al. [29] has investigated the phase transformation of Ti-6Al-4V alloy under different ET processes, and found that it only take 6 s to form the coarsen basket weave structure at the temperature of 806 °C. To complete the phase transformation by heat treatment, it has to take 15 min at high temperature of 980 ± 5 °C. Ma and his coworkers [30] have observed nanocrystalline γ-Fe in the cold-rolled commercial 22MnB5 boron steel resulting from ET. The steel consisting of the nano-grains of γ-Fe and the lath martensitic possesses excellent comprehensive mechanical properties. Xie et al. [31] have studied solid phase transformation of Ti-55531 near-β titanium alloys induced by electroshock treatment. As shown in Figure 1, the α phase along the trigeminal grain boundaries, which was originally small in size, grew and distributed perpendicular to the grain boundary after ET.

Some materials scientists were devoted to making materials and alloys phase transformations by electric fields to combine with other energy fields. Combining ET and heat treatment, the low carbon steel with the ultrafine-grained microstructure was obtained by Zhou et al. [32], and their strength has promoted to nearly double without decrease in ductility compared with that only treated by heat treatment. By the combination of ET and the compression deformation process, Zhao et al. [33] studied the microstructure evolution of Ti-6Al-4V alloy and found an obvious dynamic spheroidization at the relatively low temperature. The study results of Li et al. [34] revealed that ET can increase the elongation of

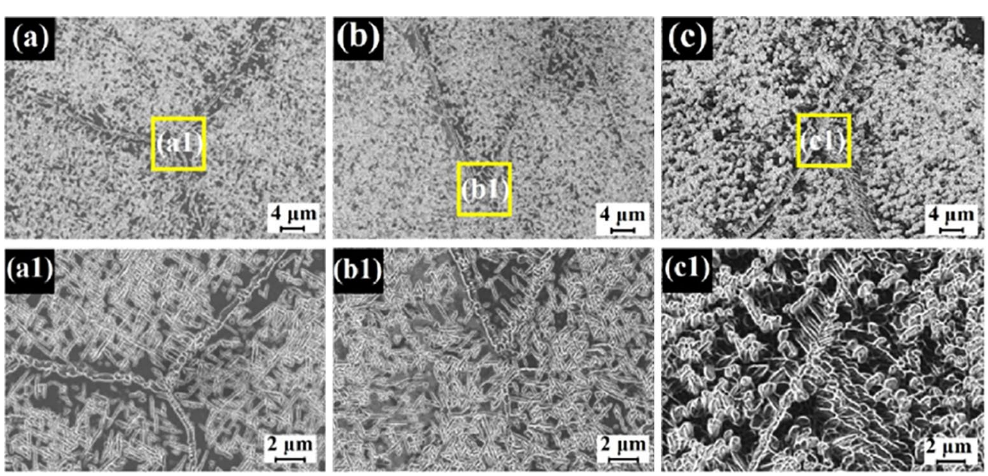

Figure 1 Microstructure of the trigeminal grain boundaries under different ET times: (**a**) 0 s, (**b**) 0.02 s, (**c**) 0.03 s [31]

SUS304 stainless steel due to the decrease of dislocation density and dislocation pile-ups and enhance its strength as a result of the promotion of martensite transformation during ET tension.

2.1.2 Effects of ET on Nano Phase Solid Solution and Precipitation

There are different functions for solid solution to different alloys. For aluminum alloy, solid solution can improve the formability of material, and affect the subsequent aging strengthening. As a key procedure to obtain excellent comprehensive mechanical properties, solid solution by ET was widely investigated to replace thermo solution in recent years. Zheng et al. [35] also found that electropulsing solution treatment could refine the grain size of 6061 alloy, but higher supersaturation degree is detected by X-ray diffraction (XRD) analysis compared with thermo solution. Figure 2 shows that the sample treated conventional solution treatment (CST) at 530 °C has more residual phases than that treated by ET at the same temperature. Similarly, Xu and his co-workers [36] have studied the solid solution treatment in 7075 Al alloy by ET. It was found that solid solution by ET could obtain finer grains, but the elongation of the alloy after ET solution is slightly lower in comparison with thermo solution resulting from the more undissolved second-phases. In addition, Wu et al. [37] have proposed a double electroshock treatment strategy, which can improve the elongation of Al–Zn–Mg–Cu alloys after ET solution.

In addition to aluminum alloy, the dissolution of phases induced by a current was also found in other alloys. Jeong et al. [38] have researched the tensile deformation behavior of extruded AZ91 Magnesium Alloy under pulse current. By comparing the electric pulse drawing and the conventional heat treatment drawing under the same conditions, it is found that the current accelerates the dissolution of $Mg_{17}Al_{12}$ phase in magnesium alloy. Tang and his coworkers [39] have discovered that the pulse current accelerate the dissolution of β phase in AZ61alloy at relatively low temperature.

High-density current could generally lead to solid solution, while low-density current is able to promote precipitation. Liu et al. [40] have found that the low-density pulse current can promote the growth of the precipitate θ' phases in the supersaturation 2219 aluminum alloy. Wang et al. [41] treated 6061 aluminum alloy specimens after conventional solid solution treatment (550 °C, 1 h, water quenching) by electric pulse aging (current density 6.643×10^{7} $A\cdot m^{-2}$, 50 V, 6–10 h). It was found that electric pulse aging can promote stable precipitation of Al_5FeSi phase compared with traditional solid solution aging process.

The effect of direct current upon interfacial reactions in the Ni–Ti system was investigated by Garay et al. [42]. Isothermal diffusion couple experiments were conducted under varying current densities to de-couple Joule heating from intrinsic effects of the current flux. Current densities of up to 2546 $A\cdot cm^{-2}$ were used in the temperature range of 625–850 °C. All of the intermetallic compounds (NiTi, Ni3Ti and NiTi2) present in the equilibrium phase diagram were identified in the product layer. In addition, β-Ti solid solutions formed in samples annealed above the α→β temperature, 765 °C. The growth of all product

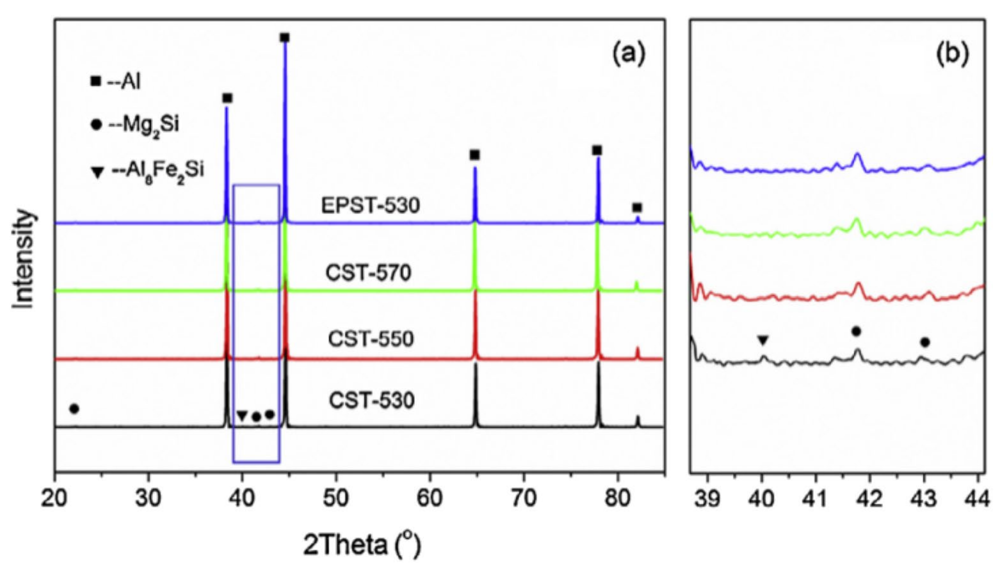

Figure 2 (**a**) XRD patterns of the ET and CST samples, (**b**) Magnification of the rectangular area in (**a**) [35]

layers was found to be parabolic and the applied current was found to significantly increase the growth rate of the intermetallic layers. Using Wagner's analysis the present results were compared to published results on current-free diffusion couples. The intrinsic growth rate constant of the NiTi2 intermetallic was found to be 43 times higher under the influence of 2546 A·cm^{-2} than that obtained without a current at 650 °C. The effective activation energy for the formation of all phases was found to decrease with increasing current density. The effect was strong for all phases but the decrease was most marked for Ni3Ti. In this case, the activation energy decreased from 292 kJ·mol^{-1} under the influence of a current density of 1527 A·cm^{-2} to 86 kJ·mol^{-1} when the current density was 2036 A·cm^{-2}. The results are explained in terms of current induced changes in the growth mechanism arising from changes in the concentration of point defects or their mobility.

2.1.3 Mechanism of Phase Evolution Induced by ET

When the current passes through the solid metal materials, the Joule heat which is considered to be the main cause of phase transition and precipitation during ET is produced in the materials. However, there are some the differences between Joule heat and conventional heat sources, which are mainly manifested in the following aspects.

Firstly, as a result of the different conductivity of nucleus and parent phase, the temperature field produced by current is unevenly distributed in micro scale [30]. As shown in Figure 3, when a new phase with high conductivity nucleates in the parent phase, its local current density is much higher than the overall current density of the sample. The difference in temperature ΔT due to the uneven distribution of current density $j(t)$ can be expressed as follows [43]:

$$\Delta T = \frac{\int_0^{t_d} \rho j^2(t)\mathrm{d}t}{c_p d}, \tag{1}$$

where ρ represents the resistivity of the material, t_d represents the electrifying time, C_p and d represent the heat capacity density of the material is of the material. Large local overheating degree of the material, accordingly, promotes the rapid nucleation and growth of new phases in local region.

Secondly, when a high-frequency current treated the materials is loaded, the induced current, its distribution decreases gradually from the center of the material to the outer surface and its direction always counteracts the loading current, will be generated inside the material, so the current tends to accumulate on the surface of the material. This skin effect of electric current will lead to the phenomenon that the Joule heat on the surface of the material is higher than that at the center of the material [44]. Skin thickness δ can be calculated by the following formula:

$$\delta=\sqrt{\frac{\rho_e}{\pi\mu f}}, \tag{2}$$

where ρ_e and μ are the conductivity and permeability of materials, respectively, f denotes the loading frequency of

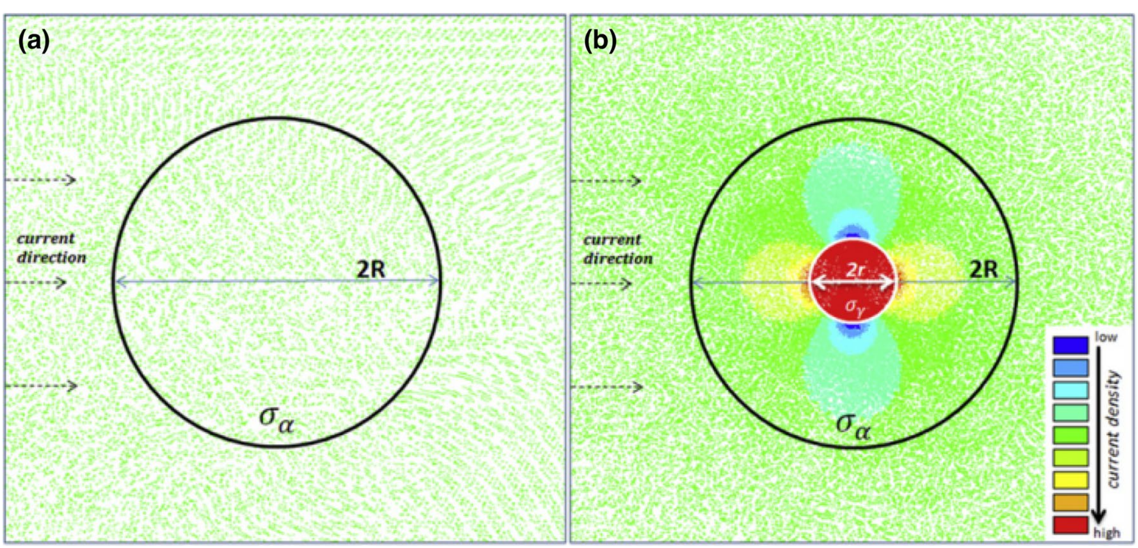

Figure 3 Qualitative numerical simulation result of the current density distribution when an electric current passing through (**a**) a α-Fe sphere of radius *R* and (**b**) that with a γ-Fe nucleus of radius *r* (*r* << *R*) at the center by Ansys, where the conductivity $\sigma_\alpha < \sigma_\gamma$ (the dashed arrows denote the current direction) [30]

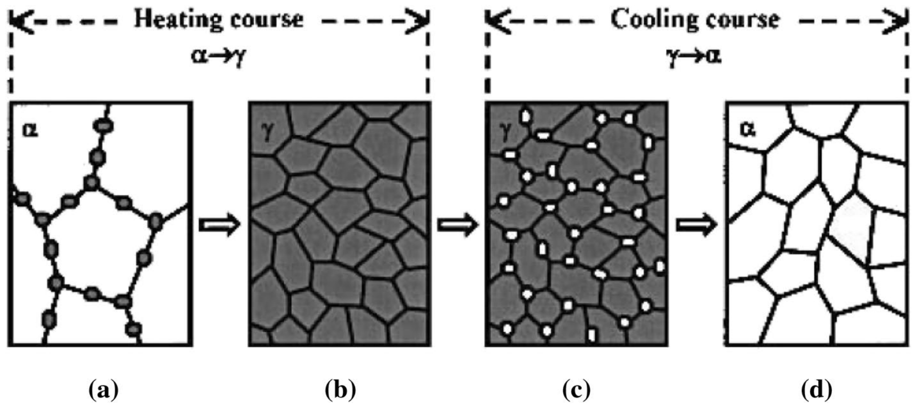

Figure 4 Schematic illustration for grain refinement and UFG microstructure formation: (a) Formation of γ-phase nuclei, (b) Formation of γ-phase grains by the growth of γ-phase nuclei, (c) Formation of α-phase nuclei, and (d) Formation of α-phase grains by the growth of α-phase nuclei [32]

power. But up to now, little research has been reported on the effect of skin effect on materials phase transition.

Finally, comparing with the conventional heat treatment, the ET has the characteristics of fast heating speed and short duration. The sharp rise and fall of temperature in a relatively short time result in the high nucleation rate and short the grain growth time in the materials. This method contributes to refine the grain size of materials and formed materials with excellent strength and toughness. Based on this rule, Zhou et al. [32] have proposed cyclic solid phase transformation mechanism to refine grain size of low carbon steel. As shown in Figure 4, a great quantity of nucleation and growth of γ phase arises at the grain boundary of α phase, and refined α phase is formed during subsequent cooling process.

In addition to the Joule heating effect, the current also causes the decrease of nucleation barrier [45, 46]. If a spherical nuclei with small volume is formed at the initial stage of nucleation, the reduction of nucleation barrier caused by its current can be expressed as [47]

$$W_e = K_1 j^2 \zeta V, \tag{3}$$

where K_1 is a constant related to the properties of materials, j and V denote the current density and the volume of the nucleation respectively. ζ can be written as $\zeta=(\sigma_0-\sigma_n)/(2\sigma_0+\sigma_n)$, where σ_0 and σ_n are the conductivity of the matrix and nucleus. When the resistivity of the matrix is greater than that of the nucleus, $\zeta>0$, $W_e>0$, the nucleation barrier increases, whereas the nucleation barrier decreases. The decrease of nucleation barrier causes the increase of the driving force of phase transition and nucleation rate at the same temperature. The reasons of grain refinement caused by ET have explained by this rule in some papers [32, 48]. Meanwhile, it can also interpret the change of phase transition temperature [47].

$$I = I_r \times \exp\left[-\frac{W_e}{K(T+\Delta T)}\right], \tag{4}$$

where I_r denotes the nucleation rate without current, K is the Boltzmann constant. According to Eqs. (1) and (3), W_e is independent of pulse duration, while ΔT is a function of pulse duration. If the pulse duration is long and the current density is low, ΔT is large and W_e is small, So the effect of EPT on nucleation rate is mainly reflected in Joule heat efficiency. Conversely, if the material is treated with high current density for a relatively short time, ET mainly reflects the change of nucleation barrier.

2.2 Effects of ET on Recovery and Recrystallization

Due to plastic deformation, larger internal stress emerges within the metal materials as a result of the distortion of lattice and the fragmentation of the grains. ET can facilitate the recovery and recrystallization of the metal in this state, and its effect is different from that of traditional heat treatment in some respects.

Firstly, finer recrystallized grains can be obtained by ET. Xu et al. [49] studied the recrystallization of 2024 aluminum alloy after hot rolling by ET. It was found that the recrystallized grain could be refined obviously when the current density is 200×10^6 A·m^{-2} and the duration is 240 ms. As shown in Figure 5, the average grain length after ET decreases from 277 μm to 11 μm compared with that under hot roll pressing. Similarly, Liu et al. [50] investigated the recrystallization of Mg-3Al-1Zn after hot rolling under pulsed current, and discovered that current accelerated recrystallization and refined the microstructure. Conrad et al. [51, 52] researched the recrystallization of cold-deformed metal materials such as copper and aluminum by ET. The results suggested that fine recrystallized grains could be formed when appropriate ET parameters (frequency and duration) were applied.

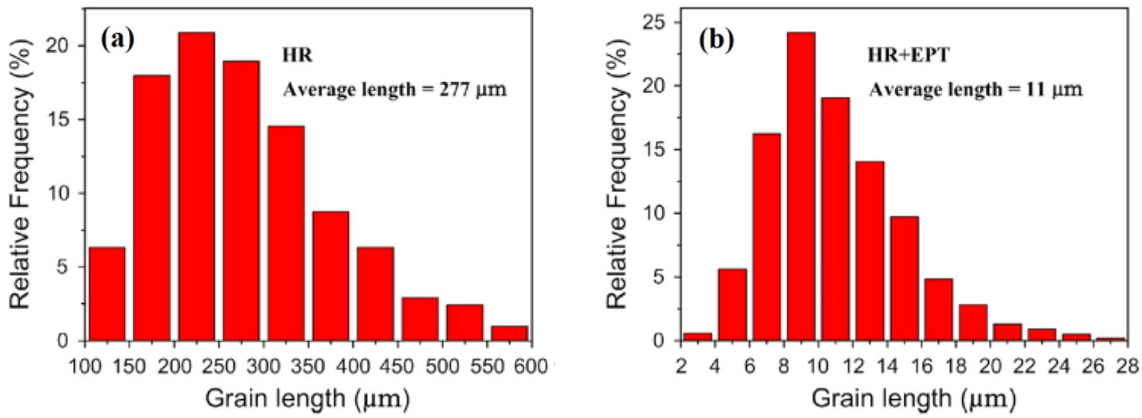

Figure 5 Effective grain length distribution with different conditions: (**a**) HR, (**b**) HR+ET [49]

Secondly, ET can make recrystallization take place at lower temperature by comparison with traditional heat treatment. Compared the recrystallization behavior of NiTi treated by heat treatment and ET, Zhu et al. [53] found that ET could reduce the recrystallization temperature by 200 °C. Similarly, Liu et al. [54] found that when the pulse current frequency was 400 Hz, the recrystallization temperature of NiTi alloy was approximately 427 °C, while the recrystallization temperature during heat treatment was 550–600 °C. When Lin et al. [55] studied the tensile test of AZ31 magnesium alloy, the results indicated that the dynamic recrystallization temperature of AZ31 alloy was 200 °C, and dynamic recrystallization could occur at room temperature after loading 150 Hz/50 V pulse current.

The main mechanisms for these differences are summarized as follows. Some researchers [50, 56] proposed that the reasons of the increase of the nucleation rate and the reduction of recrystallization temperature is attributed to the change of nucleation barrier W_e due to the current shown in Eq. (3). Some [39, 56] suggested the athermal effect of current increase the flux of the diffusion atoms and accelerate the dislocations climbing.

$$J_a = \frac{2N \cdot D_l \cdot Z^* \cdot e \cdot \rho \cdot j_m \cdot t_d}{\pi KT}, \tag{5}$$

where D_l and N denote the lattice diffusion coefficient and the density of atom respectively, Z^* and e are an effective valence and the charge on an electron respectively, j_m and f are peak current density and frequency, respectively. It can be seen from Eq. (5) that increasing peak current j_m and duration of current t_d can promote atomic diffusion and nucleation. In addition, Conrad et al. [57] analyzed that ET could promote nucleation, refine grains and reduce recrystallization temperature from the point of view of electron wind promoting dislocation movement.

2.3 Effects of ET on the Dislocations Evolution

Although the underlying mechanism of the phenomena mentioned above cannot be completely attributed to the Joule heat effect, these phenomena are hardly observed in the materials if there is no high temperature in the process of ET. However, Dislocation evolution induced by the current seems to occur at the case of relatively low temperature rise. Kim et al. [7] discovered that when the pulse current flows through the aluminum alloy under uniaxial tension, the formability of the alloy could be considerably improved. By comparing the specimens with and without pulse current, it is found that the dislocation density of the specimens with pulse current is greatly lower than that without pulse current. When X80 pipeline steel was treated by high density current, Xiang et al. [58] found that the current can promote the extinction of dislocations and the dislocation arrangement tends to the direction of electron motion. Zhu et al. [59] also observed that the dislocations inside the grain are arranged in the similar orientations by the ET with a certain process condition.

Zhao et al. [60] have investigated the dislocation evolution of pre-deformed Ti–Al alloy specimens after ET. As shown in Figure 6, the method of dislocation movement is mainly planar slip during deformation of Ti–Al alloy at room temperature, so the dislocations are aligned and relatively straight aft deformation in Figure 6(a) and (b). The researchers believe that the pulse current could cause the dislocation either depinning from the discrete obstacles or cross slip onto adjacent planes. It could be observed in Figure 6(c) and (d). That distribution is more

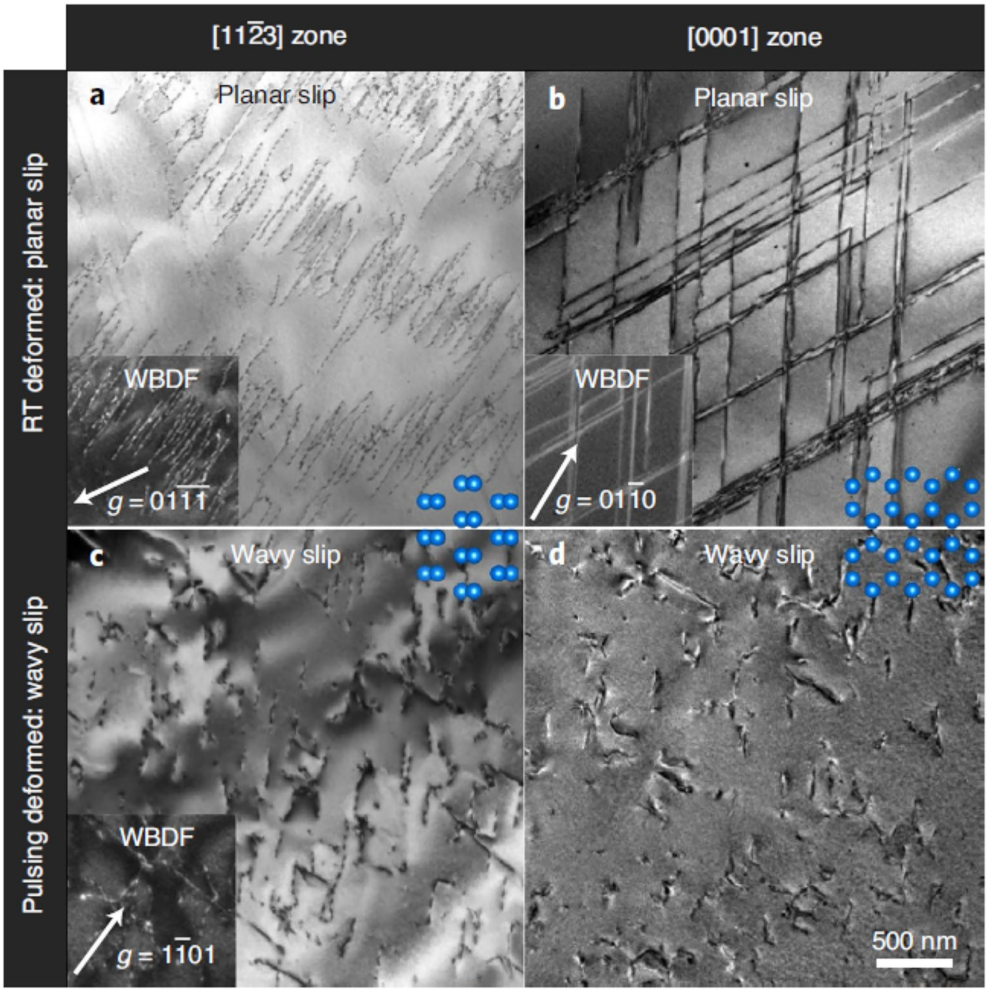

Figure 6 Dislocation morphology images of pre-deformed Ti-Al alloy specimens: Bright-field Transmission Electron Microscope (TEM) image without ET (**a**) from [11$\bar{2}$3] zone axis and (**b**) from [0001] zone axis; (**c**) and (**d**) are images with ET and the imaging conditions are correspond to those of (**a**) and (**b**) (The two beam, weak beam dark-field images are inset in the corresponding bright-field images) [60]

homogeneous and a large number of jagged dislocations exist in the pulsed sample.

There is no unified perspective on the mechanism of dislocation motion caused by an electron current [8, 28]. As the first mechanism proposed to interpret the effect of electroplastic effect, the electron wind force refers to the drag force arising from electrons in directional motion on dislocations [58]. This interpretation has been unanimously recognized by scholars for more than 30 years, but with more accurate theoretical calculation, it has been found that the electronic wind force is one to two orders of magnitude smaller than enough to drive dislocations [61]. Subsequently, Russian scientists proposed the dislocations depinning model induced by current magnetic effect [62] and hot dislocation model [63]. However, it seems that these standpoints have not been verified by experiments.

2.4 Effects of ET on Defects Healing

In order to improve the fatigue life of materials, the method of crack healing by ET has attracted increasing attention due to its advantages of time-saving, well healing effect and little influence on other parts of the matrix [64, 65]. Figure 6 is the scanning electron microscope (SEM) photographs of the fatigue cracks before and after ET [66]. By comparison with Figure 7(a) and (b), there are obvious bridging and healing phenomena of cracks after ET. Indeed, similar phenomena are discovered not only in steel, but also in aluminum alloy [67], titanium alloy [68] and copper alloy [69].

Joule heating effect is the main reason for crack healing caused by ET. Compared with other heat sources, Joule heating effect has its own characteristics. When a current field is applied to a specimen, the inhomogeneous electric density distribution is caused by the internal defects of

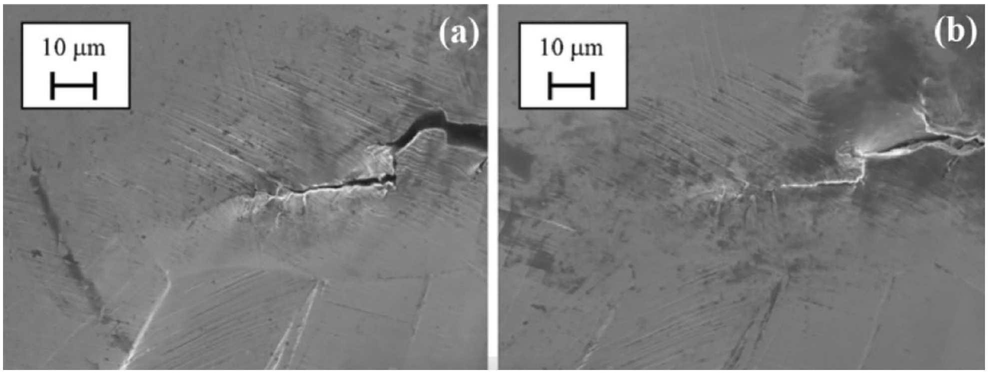

Figure 7 SEM photographs of the fatigue cracks in specimen: (**a**) before and (**b**) after the application of the ET [66]

materials such as dislocations, heterogeneous phases and cracks. The current density j at the elliptical defect can be derived from Maxwell's formula, which is expressed as follows [70] :

$$j = j_0 \times f(a, b), \tag{6}$$

where j_0 denotes the current density amplitude at the defect-free region, a and b represent the size of the long and short axes of the elliptical defect respectively, among $a >> b$. When electrons directionally moving pass through defective lattice lattices, the vibration frequency and energy of atoms increase and result in higher temperature at the defective region. A research shows that the fastest-growing regions of the temperature are the middle section and the crack tip of the elliptical defects, and the maximum temperature can reach more than five times of that of the other parts in the material, and even make the material melt locally [70]. Therefore, compared with traditional heating methods, Joule heating effect has a "targeting effect" on defects at micro-scale.

Due to the increase of local temperature, there are two main positive effects on cracks healing. On the one hand, the atomic diffusion coefficient D can be expressed as follows [57]:

$$D = D_0 \exp(-\frac{Q}{RT}), \tag{7}$$

where D_0 denotes a constant, Q denotes the diffusion activation energy and R denotes the ideal gas constant. According to the above formula, the atomic diffusion ability of defective region increases with the increase of temperature. On the other hand, the temperature difference between the matrix and the defect leads to the relative expansive compressive stress and the thermal compressive stress $\Delta\sigma$ caused by the thermal expansion lagging behind the temperature [64]:

$$\Delta\sigma(t) = E\alpha \cdot \Delta T_{\max}[\Theta(t) - l(t)], \tag{8}$$

where E is the modulus of elasticity and α is the thermal expansion coefficient of the material. $\Theta(t) - l(t)$ is a function used to react the synchronization of temperature rise and expansion. When the reaction temperature rises slowly, $\Theta(t) - l(t) = 0$, there is no thermal compressive stress. While the temperature rises rapidly, $\Theta(t) - l(t) \neq 0$ the thermal compressive stress is produced, and its value increases with the increase of heating rate. Joule heat can almost maximize the thermal compressive stress $\Delta\sigma_{\max} = E\alpha\Delta T_{\max}$. The molten liquid metals around the cracks are forced by the compressive stress into the cracks, and then intense atomic diffusion causes rapid fusion of materials. When the pulse current is stopped, the cracks in the material are healed.

3 Effects of MT on Microstructures of Solid Metals

3.1 Effects of MT on the Phase Transformation and Precipitation

According to the basic theories, there are some the differences on the magnetic properties among the different precipitation phases or the same precipitation phases at different temperatures. For instance, ferrite is paramagnetic above Curie temperature and ferromagnetic below Curie temperature. Additionally, the magnetic field could also affect the nucleation and growth of new phase during phase transformation process by changing the atomic diffusion coefficient. In recent years, some scholars have studied heat treatment in strong magnetic field. The relevant experiments have indicated that the effect of strong magnetic field on phase transformation process is mainly reflected in the change of the transformation temperature, the morphology, texture and mass fraction of phase transformation products.

3.1.1 Effects of MT on the Transformation Temperature

A large number of studies have shown that the magnetic field has a significant effect on the phase transition temperature [71–74]. The decomposition temperature of austenite (A_{r1}, T_p and A_{r3}) increases with the increase of magnetic field intensity [75]. The martensite transformation temperature of the alloy steel (mass fraction 0.3% C, 3% Ni and 0.6% Cr) quenched in 16 kG magnetic field moves about 5 °C in comparison to without magnetic field [76]. When ferrite transforms to austenite, the temperature of A_{c1} and A_{c3} increases with the increase of applied magnetic field intensity, but the temperature of A_{cm} is hardly affected by applied magnetic field [77].

Liu et al. [78] reported the adiabatic temperature change $\Delta T_{ad} = -3.6$ to -6.2 K under a moderate field of 2T for Heusler-type Ni–Mn–In–(Co) magnetic shape-memory alloys. Reversible martensitic transformations induced by magnetic field in NiCoMnIn meta-magnetic shape memory alloys under constant and varying mechanical loads were studied by Bruno et al. [79]. They Measurements revealed that these meta-magnetic shape memory alloys were capable of generating entropy changes of 14 $\mathrm{J{\cdot}kg^{-1}{\cdot}K^{-1}}$ or 22 $\mathrm{J{\cdot}kg^{-1}{\cdot}K^{-1}}$, and corresponding magnetocaloric cooling with reversible shape changes as high as 5.6% under only 1.3 T or 3 T applied magnetic fields, respectively. And they demonstrate that this alloy is suitable as an active component in near room temperature devices, such as magnetocaloric regenerators, and that the field levels generated by permanent magnets can be sufficient to completely transform the alloy between its martensitic and austenitic states if the loading sequence developed.

The effect of magnetic field on phase transition temperature can be attributed to the change of Gibbs chemical free energy in parent phase and new phase by magnetic field [80–82]. This change is caused by the energy of both the magnetostatic effect and forced volume magnetostriction effects. When the material is non-Invar alloys, the forced volume magnetostriction effects is less significant and can be ignored. Compared with phase transition without magnetic field, the variation of phase transition temperature ΔT with magnetic field strength H can be written as [81]

$$\Delta T = -\frac{1}{\Delta s}\int_0^H \Delta M \mathrm{d}H, \tag{9}$$

where Δs is the change of entropy and ΔM is the change of magnetization. If the relationship between the change of entropy and magnetization and magnetic field intensity H can be measured, the variation of phase transition temperature ΔT can be calculated. The variation of magnetization can be roughly calculated by molecular field theory, however the results obtained by Faraday method are more accurate when the material temperature is near Curie point [75, 83].

3.1.2 Effects of MT on the Morphology and Volume Fraction of Phase

The magnetic field also has a great influence on the composition and morphology of the phase transformation products. by comparison experiment, it is found that Fe-0.4C alloy is equiaxed ferrite without magnetic field during the transformation of isothermal ferrite, but the grains grow along the direction of magnetic field and the grains are elongated with 10 T magnetic field, and the degree of elongation increases with the increase of magnetic field strength [84]. Shimotomai et al. [85] discovered that the austenite grains of Fe–C alloy in the pre-eutectoid ferrite matrix aligned as chain or columns shape along the direction of magnetic field during the transformation from ferrite to austenite. As shown in Figure 8, Zhang et al. [86] found that the morphology of carbides in structural steels tempered at 650 °C for 1 h is lamellar in the absence of magnetic field, while it is mainly granular in 14 T magnetic field.

Similarly, the magnetic field also obviously affects the volume fraction of the product. Table 1 summarizes the effect of magnetic field on the volume fraction of phase

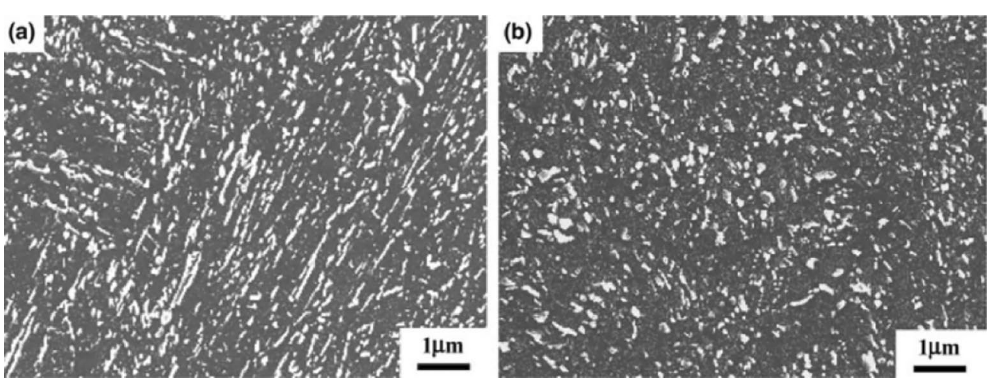

Figure 8 SEM micrographs of carbides obtained by tempering at 650 °C for 1 h (**a**) without field, (**b**) with a 14 T magnetic field (field direction vertical, SEM secondary electron images) [86]

Table 1 Summary of reported strong magnetic field effects on morphology and amount of produced phase

Materials	Magnetic flux density (T)	Produced phase	Differences of volume fraction	Refs.
TC4 titanium alloy	4	α phase	Increase by 20%	[87]
Cu–72 wt% Ag alloy	12	Lamellar Cu	Decrease by 1.4%	[88]
Ni42Co8Mn39Sn11 alloy	12	Martensitic	Increase by 0.45%	[89]
Fe-1.1%C alloy	12	Secondary cementite	Increase from 0.62% to 1.54%	[90]
Al–4.8%Cu alloy	11.5	θ phase	Decrease from 6.8% to5.2%	[91]
Fe-0.5C3.6Ni1.5Cr alloy	10	Bainitic	Increase from 8% to 97%	[92]
7085 aluminum alloy	12	T and S phase	Significantly decreases	[93]
Fe-0.44C0.23Si1.2Mn alloy	10	Ferrite	Increase by 10%	[94]
Alnico alloys	10	Ferromagnetic particles	Significantly increases	[95]

change products of different materials. From this table, it can be seen that the magnetic field has a significant effect on the phase transformation composition of ferromagnetic and non-ferromagnetic materials. Therefore, through adjusting the magnetic field intensity, heat treatment can effectively control the volume fraction of the product, thus regulating the properties of the material.

The effect of magnetic field on the morphology of the new phases can be accounted for the anisotropy of atomic magnetic moment and grain magnetization energy, etc. [96–99]. However, existing explanations for the variations of the mass fraction of the formed phase in magnetic field are roughly summarized as follows.

During the phase transition, the change of the free energy ΔG_{mag} can be expressed as $\Delta G_{\text{mag}} = -\int_0^H \Delta M \mathrm{d}H$. In one case, both ferromagnetic and non-ferromagnetic materials are transformed into each other during the phase transformation process, due to the great difference for the magnetic susceptibility of ferromagnetic and non-ferromagnetic materials, the influence of magnetic field on the free energy before and after phase transformation is great. Thus, the nucleation barrier and the growth rate of the new phase in the phase transition process are altered, and then the mass fraction of the formed phase is altered [100]. In another case, for non-ferromagnetic materials, the driving force ΔG_{mag} of magnetic field on phase transition is small. However, the magnetic field perhaps promotes the diffusion coefficients of specific elements, enhances the phase transitions and increases the volume fraction of specific phases.

3.2 Effects of MT on the Texture Formation of Solid Metals

Due to the diversity of grain characteristics in difference directions, when all the lattices tend to align uniformly, the material exhibit anisotropy macroscopically. The anisotropic functional material plays an important role in practical application. When the permeability of crystals is anisotropic along the axis, both ferromagnetic and non-ferromagnetic materials can form texture in a sufficiently strong magnetic field [101]. For ferromagnetic and paramagnetic materials, the crystal axis of the maximum susceptibility tends to be parallel to the direction of magnetic field, while for diamagnetic materials, the direction with the maximum absolute susceptibility tends to be perpendicular to the direction of magnetic field.

As a result of anisotropy of permeability, the magnetic alignment is generally obtained in non-cubic structure. *c*-axis of tetragonal MnBi crystals is parallel to the applied magnetic field direction by rotation of MnBi particle [102]. When hexagonal Bi-5masss% Sn alloy was placed into a 12 T magnetic field, the peak value correspond to *a*, *b*-plane in X-ray diffraction spectra increases obviously [103]. However, the intensity of *c*-axes of Zn crystals toward <0 0 2> direction increases with the increase of magnetic field intensity in eutectic BiZn structure [104].

Feng et al. [105] reported the formation of single crystals with rigorously controlled texture over macroscopic areas (> 1 cm^2) in a soft mesophase of a columnar discotic liquid crystal, they use two modes of directed self-assembly, physical confinement and magnetic fields, to achieve control of the orientations of the columnar axes and the hexagonal lattice along orthogonal directions, their research shows that the field control of the lattice orientation emerges in a low-temperature phase of tilted discogens that breaks the field degeneracy around the columnar axis present in non-tilted states.

The main reasons of magnetic texture are summarized as follows. Firstly, from the thermodynamic point of view, because of the anisotropy of susceptibility of crystal orientations, when the magnetization energy difference is greater than the thermal energy, it provides conditions for the formation of magnetic texture. This relationship can be written as [103, 104]:

$$|\Delta U| = |U_c - U_{a,b}| = \left| -\frac{(\chi_c - \chi_{a,b})}{2\mu_0(1 + N\chi_{a,b})(1 + N\chi_c)} B^2 \right| > \frac{kT}{V}, \tag{10}$$

where V is the particle volume, k and μ_0 denote Boltzmann's constant and the vacuum permeability respectively. T is the absolute temperature and ΔU is the change value of magnetic field energy. N is the demagnetization coefficient. χ_c and $\chi_{a,b}$ are the susceptibility along the c axis and a,b axis respectively, and B is the magnetic induction intensity. In the case of paramagnetic materials, when $\chi_c > \chi_{a,b}$, the grain nucleation and growth tend to be parallel to the direction of magnetic field on the c-axis. When $\chi_c < \chi_{a,b}$, the c-axis of the grain tend to be perpendicular to the direction of the magnetic field. These phenomena, such as Aluminum plates (0 0 l) aligned in the direction of magnetic field [106], and the easy magnetization axis of Al_3Ni crystal oriented parallel to the imposed magnetic field sand the primary phase Al_3Ni aligned perpendicular to the magnetic fields [107], are well explained.

Secondly, from the magnetic moment point of view, when the direction of magnetization of anisotropic magnetic grains is disagree with that of magnetic field, the magnetic moment K can be expressed as follows [108]:

$$K = \frac{\Delta\chi}{2\mu_0} B^2 V \sin 2\alpha, \tag{11}$$

where $\Delta\chi$ is an anomaly of magnetic susceptibility, α is the angle between the direction of magnetic field and the direction of maximum magnetization axis. Assuming that $\chi_c > \chi_{a,b}$, as shown in Figure 9, when the c-axis is not parallel to the direction of the magnetic field, the magnetic moment acting on the grain causes the grain to rotate. Until the c-axis is parallel to the direction of the magnetic field, the magnetic moment K is zero, and it will remain stable.

In addition, the magnetic field drives the grain boundaries of magnetic susceptibility anisotropic materials [109]. This driving force can also lead to preferred orientation growth of grains. This theory has been used to interpret the effect of the strong magnetic field on the texture evolution in titanium alloys and the annealing texture in cold rolled pure zirconium [110, 111]. Finally, Zhang et al. [99], from the perspective the dipolar interaction of the magnetic moments, has well explained the texture formation in the medium plain carbon steel during the diffusional decomposition of austenite.

3.3 Effects of MT on Dislocations Evolution

The aforementioned effects of magnetic field on microstructure of materials generally occur during heat treatment of metal materials. Nevertheless, at room temperature, magnetic field can also alter the microstructure of metal materials, which is mainly reflected in dislocation changes.

In 1965, Zagoruiko [6] proposed that high magnetic field can affect the activity of dislocation electrons, promote the movement of dislocations and enhance the plasticity of materials. As shown in Figure 10 [112], by comparing dislocation pit before and after MT, the dislocation motion can be obviously observed in situ. Subsequently, Russian scholars have made great efforts on the micro-nature of magnetic field promoting dislocation movement in alkali halide crystals (NaCl, LiF, CsI, KCl) by the method of continuous etching [113–115].

For metal materials with high dislocation density, the method of continuous etching is almost useless. a plenty

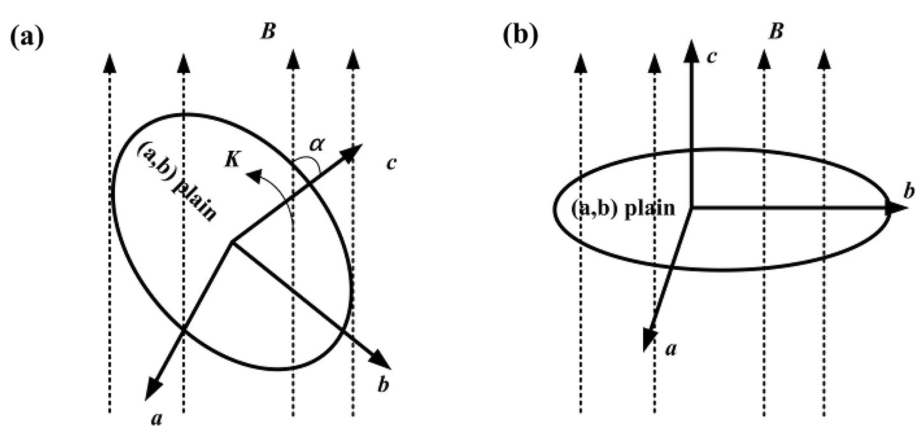

Figure 9 Schematic diagram of magnetic moment on anisotropic grains: (**a**) The magnetic field is not parallel to the *c*-axis, (**b**) The magnetic field is parallel to the *c*-axis

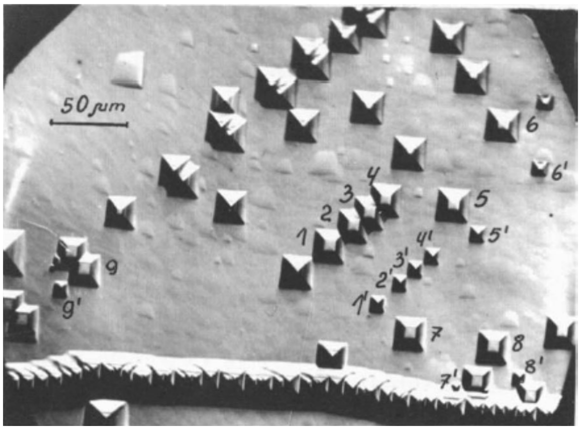

Figure 10 Dislocation motion diagram before and after MT [112] (1, 2, 3, …, 9 dislocation pit before MT; 1′, 2′, 3′, …, 9′ dislocation pit after MT)

of scholars have studied the dislocation distribution by TEM before and after MT. Many scholars from Tsinghua University have studied the changes of dislocation distribution of commercial high strength steel after MT [15, 116]. The experiment results indicate that dislocations absent from MT are mainly distributed at grain boundaries and the junction of triple grain boundaries, while the distribution of dislocations is more homogenous after MT and the dislocations cells disappeared.

Meanwhile, the variation of dislocation density after MT in metal materials has been quantitatively studied by X-ray diffraction spectroscopy. The research of Li et al. [71] shows that dislocation of TC4 titanium alloy density is 4.8 times as high as that without magnetic field, when it is stretched in 3 T magnetic field. Ma et al. [117] indicated that the dislocation density of high speed steel increases by 24% after MT. Chen et al. [118] proposed that the dislocation density at the weld can be increased by about 237.09% after MT. Song et al. [119] investigated the dislocations distribution in the heat affected zone of laser welded plates by TEM. As shown in Figure 11, the dislocation density increases significantly after MT.

The mechanism of magnetic field driving dislocation motion in metal materials is summarized as follows. Some researchers hold that the magnetic field produces shear stress on the dislocation, which can be expressed as follows [120]:

$$\tau = -\mu_0 M_s H \cos\theta, \tag{12}$$

where M_s and μ_0 denote the saturation magnetization and the permeability of vacuum respectively, H denotes the magnetic field intensity, and θ denotes the angle between the direction of magnetization and the magnetic field. This stress is greater than the P–N forces acting on dislocations and the elastic strain forces bending dislocations, therefor the dislocations can be driven by magnetic fields [117]. Some considered that the magnetic field which transforms the spin state of the radical pairs from the ground singlet (S) state to the excited triplet (T) state, prompt the dislocation depinning from the paramagnetic barrier, and then internal stress and thermal potential energy in material advance the dislocation motion [12, 121–124]. While others argued that when there is internal stress in the material, the dislocation in the local region can be facilitated by the interaction of internal stress and magnetostriction during MT [125].

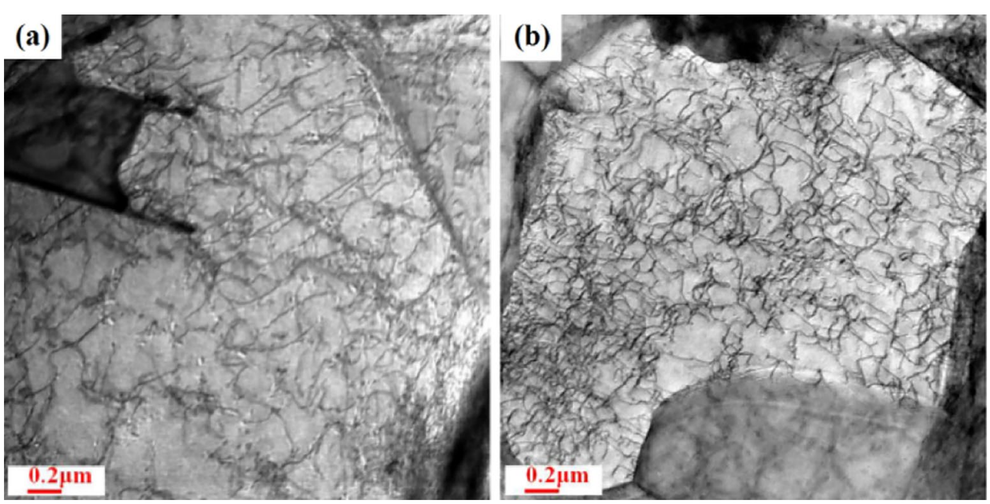

Figure 11 Dislocation distribution of DP600 steel in heat affected zone of laser tailor welded blanks (a) absent from MT, (b) with MT [119]

3.4 Other Phenomena Related to MT

Atomic diffusion plays a crucial role in numerous kinetic processes in alloys, e.g., homogenization, creep and corrosion. Over the past decade, it has been confirmed that applying external magnetic field can affect the atomic diffusion rates of the alloying elements, e.g., Ni–Cr [126], Mg–Gd [127] and Fe–Al [128]. Nevertheless, the mechanisms of the change in diffusivity in magnetic field are still not fully clear.

An intermediate frequency magnetic field (IFMF) was imposed upon Gd–Mg diffusion couples that were annealed at 773 K [127]. It was found that the average thickness of diffusion layer under the magnetic field was much wider than that without the magnetic field, indicating that the atomic diffusion ability was enhanced. The magnetic field was then applied to the solution treatment of Mg–16.66Gd–0.088Zr (wt%) alloy. Compared with the samples without magnetic field, the area fraction of the eutectic phase (Mg 5 Gd phase) was evidently lower at each time point when the IFMF was imposed during the solution treatment, i.e., the solution treatment process was accelerated by the magnetic field.

A novel welding method was proposed by Chen [128] to realize the connection between the stainless steel 301 and the aluminum alloy with a steady magnetic field perpendicular to the welding direction. The mechanical properties were thoroughly investigated to discuss the function of the magnetic field in the laser welding of the steel/Al. They experimental results indicated that the thermoelectric magnetic force (TEMF) induced by the interaction between thermoelectric and the magnetic field played decisive roles in the suppression of element diffusion during the welding. The reaction area between steel/Al decreased due to the diffusion of the Al atoms was suppressed, the suppression of diffusion of C and the decrement of Gibbs energy of Fe, led to an increasing of nucleation rate and decreasing of growth rate.

The MT enhances the atomic diffusion ability may be explained as the ambipolar diffusion. Metals can be treated as solid plasma that consists of free electrons and constrained positive ions, the atomic diffusion can be treated as an am-bipolar diffusion process [127]. The diffusion coefficient can be expressed as follows:

$$D = \frac{\mu_e D_i + \mu_i D_e}{\mu_e + \mu_i}, \tag{13}$$

where D is the am-bipolar diffusion coefficient, D_i and μ_e are the diffusion coefficient and the mobility of positive ions (electrons). According to Maxwell's equations, the alternating magnetic field is always accompanied by alternating electric field and this electric field can accelerate the mobility of electrons, and then the accelerated electrons can pull the positive ions to achieve a new higher equilibrium diffusion rate. Therefore, metal atoms get higher diffusion ability in magnetic field.

4 Effects of Combined ET and MT on Microstructures of Solid Metals

As yet there are few studies on combined treatment of current and magnetic field on properties and microstructure of materials [129]. However, this method has significant effects on material properties, and its effects are not simply the superposition of ET and MT. Pinchook and Shavrei's [130, 131] research on Bismuth Crystals shows that the simultaneous treatment of the current pulses and magnetic field (STCM) leads to a substantial decrease in the density of twinning dislocations piled up at the boundaries of wedge twins and an increase along

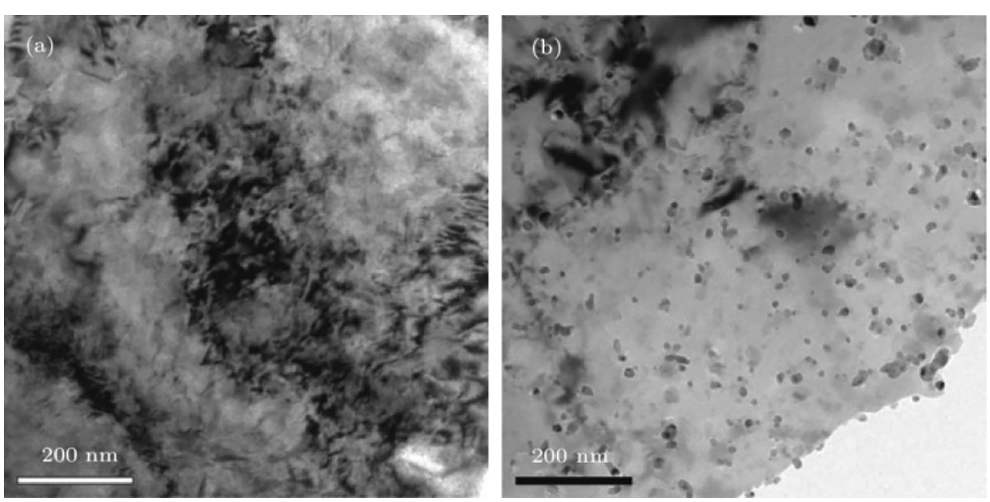

Figure 12 TEM photograph of Aging of Cu-Cr-Zr alloy at 450 °C (**a**) without magnetic field, (**b**) with 10 T magnetic field (T = 3 h, I = 100 A·cm^{-2}) [132]

the twin–matrix boundary. Rao et al. [132] studied the aging of cold-deformed Cu–Cr–Zr alloy by current and magnetic field treatment. As shown in Figure 12, the material aging at 450 °C only with ET appear obvious dislocation aggregation, while the material aging at 450 °C with ET and MT hardly occur dislocation aggregation and a large number of Nano precipitation are dispersed in the matrix. Cai et al. [129] hold that when the material are simultaneously processed by the current and magnetic field, magnetic field may provide conditions for dislocations depinning and pulsed current may provide conduction electrons to drive dislocations moving further and faster.

5 Applications of Electromagnetic Processing

5.1 Electromagnetic Force Forming

Electromagnetic force forming (EMFF) is a technology whereby large electromagnetic forces are imparted to a conductive metal sheet. By using a large electric current moves through a conductive coil to produces transient magnetic field which will induce eddy currents in a nearby metal sheet. The mutually repulsive electromagnetic pressure resulted between the stationary coil and the metal sheet can deform or accelerate metal sheet. Some studies have shown that electromagnetic force forming is a high-speed forming technology. It can be applied to some light metal sheet forming which is difficult formed to control springback effectively.

Lai et al. [133] developed a dual-coil system for deep drawing of the metal sheet with large drawing ratio, the EMFF system is shown in Figure 13. In addition to the conventional driving coil that generates the axial Lorentz force on the workpiece, a radial inward force in the flange region is generated by a second coil that is energized by an individual power supply. The axial force from coil 1 (conventional coil system) pushes the material from above into the cavity in axial direction. The radial pushing force generated on the flange by coil 2 to enhance the material flow of the flange the draw-in of the flange. The effectiveness of the novel system is validated by a series of experiments for deep drawing a cup of AA1060-H24 with drawing ratio of 3.25, the maximum forming depth without failure is greatly increased from 8.44 mm to 20.28 mm. It is demonstrated that with the dual-coil system the material flow of the flange can be significantly enhanced.

Cao et al. [134] discussed a novel strengthening method for mechanical linking holes based on the electromagnetic rivet (EMR) technique. The schematic of the EMR progress is shown in Figure 14. The riveting force of EMR is based on Lorentz force, which is converted by electromagnetic energy. During the EMR progress, a DC power source is used to charge the system capacitance firstly, a magnetic field around the master coil is established by the discharge from the system capacitance, and then a current in the slave coil is induced by this magnetic field, setting up a magnetic field around the slave coil. Finally, the interaction of the magnetic fields around the slave coil and the master coil generates a dynamic Lorentz's load. The dynamic load acts on the rivet in the form of stress wave through the driving head, leads to a finished rivet configuration with a high-speed loading rate.

With advantages over conventional riveting techniques, the EMR technique has been applied in the aerospace industry as an advanced joining tool. Typically, EMR exhibits obvious advantages in composite structure riveting, titanium riveting and large-size aluminum riveting and interference fit bolt installation.

5.2 Electromagnetic Assisted Forming

According to the research on the influence of electromagnetic energy field on the microstructure of metal,

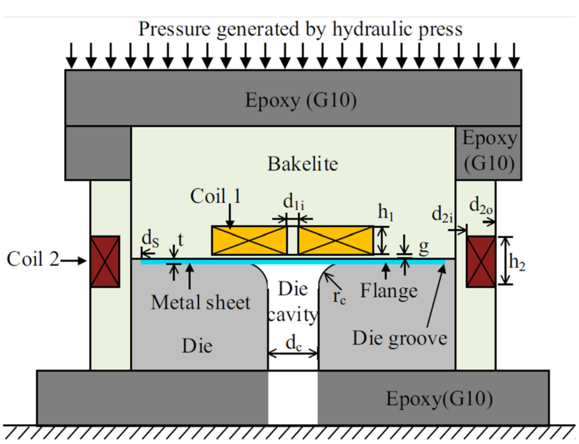

Figure 13 Schematic diagram of the dual-coil EMFF system [133]

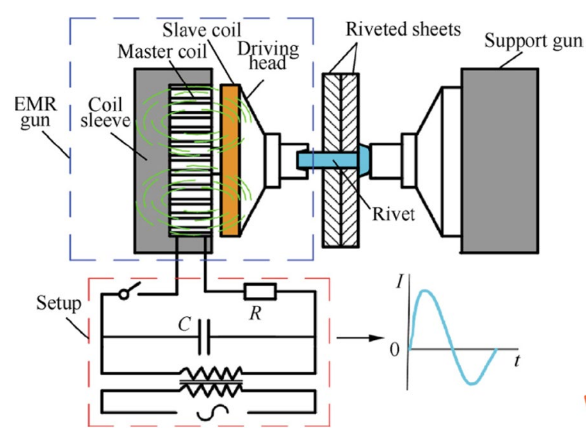

Figure 14 Schematic of the EMR progress [134]

the properties of metal will change temporarily or permanently under the action of electric field or magnetic field. Some studies have shown that electromagnetic processing technology can enhance the formability of metal in the deformation process and reduce springback after deformation, and it has the effect of reducing the internal stress and micro-cracks of materials. Combined with the common metal forming technology, some electromagnetic assisted forming methods with great application potential have been produced.

Shang et al. [135] proposed an approach called electromagnetic assisted stamping (EMAS) to improve the formability of sheet metal, which is based on the idea of directly delivering the deformation where it is required and directly controlling of strain distribution of stamped parts. By EMAS an AA2219-O sheet with diameter and thickness of 101.6 mm and 0.83 mm respectively was drawn into the shape of a cup with depth of 34.5 mm, while the cup depth obtained by conventional deep drawing without failure was only 10.4 mm. According to the research result, EMFS is expected to become an important technique for the fabrication of lightweight structures with alloys which have high strength/weight ratio, but poor formability at room temperature.

Jones et al. [136] also reported that the forge ability of Mg AZ31B-O, which is traditionally hard to forge, was significantly increased as the continuous electric current increased. The ability to form a final geometry was achievable in the EA forging process which can't be achievable at room temperature, and the overall required forces of forging decreased at higher current densities. Under the lower current densities also obtained a similar forge ability enhancement at a particularly slower platen speed. Zhu et al. [137] made Ni47Ti44Nb9 successfully rolled by electroplastic rolling at relatively low temperature compared to the traditional hot rolling. The result shows the deformability of Ni47Ti44Nb9 is improved by electropulse with the maximum thickness reduction of 24% in a single pass. And the Vickers hardness test shows electropulse can reduce the work hardening. In addition, electroplastic rolling can improve the surface quality of this metal due to the short heat treatment time and low heat treatment temperature.

Electrically assisted wire drawing process has been proved to be a feasible technique which enhances the material formability compared to the conventional wire drawing process. The electroplastic effects resulting from different electropulses configurations on a wire drawing process are investigated experimentally and numerically by Egea et al. [138] Electropulses are induced into 308L stainless steel while it is simultaneously wire drawn. A current density of 185 $A{\cdot}mm^{-2}$, a frequency range from 140 to 355 Hz and a pulse duration range from 100 to 250 μs are combined to electrically assist the wire drawing process. The results show that the wire drawing forces were reduced when the wire drawing process was electrically assisted, the formability of the material increases up to 11.9%, while the relative energy efficiency of the process improves up to 7.6% when the specimens are assisted in situ by electropulses. Moreover, the microstructure and phase determination analysis denoted that the electropulses induce a dynamic recrystallization process, a detwinning process and also an attenuation of α martensite.

Electrically assisted stretch U-bending tests have been conducted by Zhao et al. [139] to analyze the influence of electrical parameter duty cycle on the springback of Ti6Al4V sheets. It is found the introduction of electric pulses can effectively relieve springback effect of TC4 and provide an alternative method to traditional hot forming process in realizing precise manufacturing of TC4. The experiment proved that electric pulses with 75 $A{\cdot}mm^{-2}$ (effective current density Jeff is 41.1 $A{\cdot}mm^{-2}$) can reduce springback of TC4 by more than 50% in 30s compared to that obtained in room temperature.

The effect of electropulsing was observed during turning of steel S235 and aluminum 6060 by Hameed et al. [140]. The machinability indices such as chip compression ratio ξ, shear plane angle ϕ and specific cutting energy (SCE) are investigated by using different cutting parameters such as cutting speed, cutting feed and depth of cut during electrically-assisted turning process. It is found that the electrically-assisted turning process improves the machinability of steel S235, whereas the machinability of aluminum 6060 gets worse. Finally, due to electropluses (EPs), the chip compression ratio ξ increases during the turning of aluminum 6060 and the SCE decreases during the turning of steel S235 with the increase of the cutting speed.

5.3 Electromagnetic Shock Treatment Processing

Recently, a novel electromagnetic shock treatment (EST) process has been proposed by the authors' group. Its characteristics are limited current density energy, low-frequency and instantaneous pulse shock [141]. It has been verified that this method can significantly improve the properties of metals under the condition of very limited temperature rise and is suitable for various metals, such as steel [142], aluminum alloys [37] and titanium alloys [31, 143]. Song et al. [142] found that the residual stresses of cold rolled M50 steel be considerably decreased in the direction of transverse and rolling direction. By comparison, they also found the strength of the material remains almost unchanged, but the elongation increased significantly.

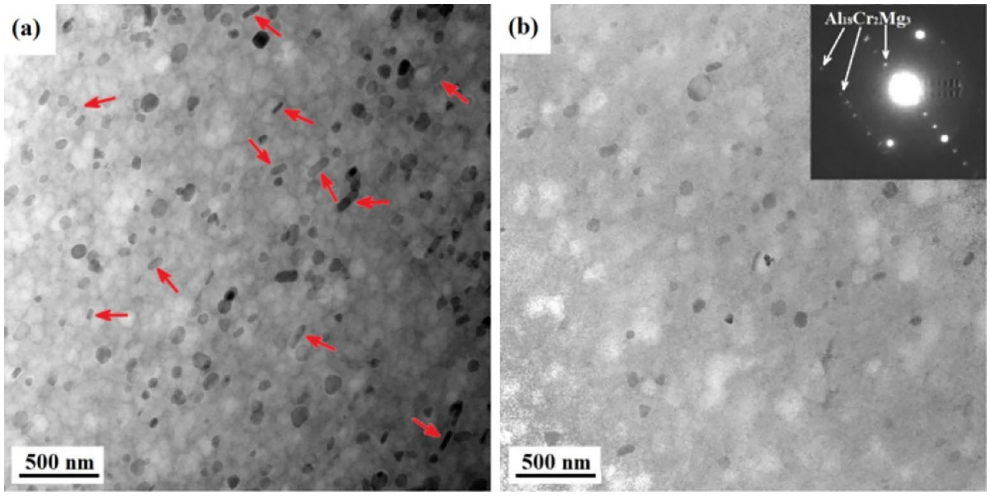

Figure 15 Bright field TEM images of the Al–Zn–Mg–Cu alloys at different states (**a**) SST, (**b**) D-EST (The red arrows point to the long rod-shape dispersion phases in (**a**) and SEDP of disperdions was inserted in (**b**)) [37]

Compared the mechanical properties of Al–Zn–Mg–Cu alloys treated by different methods, Wu et al. [37] discovered that the strength and elongation of the material treated by double electroshock treatment (D-EST) are better than those by heat solid solution treatment (SST). As shown in Figure 15, it could be found that the amount of the long rod-shape dispersions in the alloy after D-EST is significantly less than that after SST. These shape dispersions are harmful to the plasticity of the material. The reason for this phenomenon can be attributed to the non-uniform distribution of current in the micro region due to the difference of resistivity between aluminum matrix and dispersion. In addition, the authors have also found that the micro-hardness of Ti-6.6Al-3.4Mo alloys can be improved by 13.4% after EST [141].

6 Challenges in ET and MT

6.1 Multi Fields and Multi Scale Modeling

In term of theoretical research, it is obvious that the mechanism of electric and magnetic treatment is less mature relative to that of heat treatment. The influence of electromagnetic field on the motion of charged particles is clear according to Maxwell's electromagnetic field theory. In principle, based on the theory of atoms diffusion and dislocations motion by thermally activated, the theories of electromagnetic field on solid metals is able to established only by taking account of the electromagnetic force, i.e., Coulomb force and Lorentz force. However, the process is very complicated due to the non-uniform distribution of current and magnetic induction B in the micro-size of the metals. These non-uniform distributions are mainly derived from the difference of electrical conductivity and magnetic susceptibility at the microstructure. A great challenge comes from the quantitative measurement of the physical properties of the microstructure.

The mechanisms of some familiar phenomena have been controversial so far. For instance, the electronic wind force has been regarded as the mechanism of electroplastic for a long term only exists in theoretical analysis. while the superconducting condition, no Joule heat generation, is reached, the electroplastic phenomenon is absent, but electron wind force still exists theoretically at this case [144]; Furthermore, based on electromagnetic treatment experiment of aluminum single crystals, Alshits and his coworkers [145] suggested that "the nature of the "electron–plastic" effect is unlikely to have any relation to the electron drag of dislocations". For suspending these controversies, some models and simulations based on the molecular dynamics or first principles are the promising approaches to reveal the mechanism of electromagnetic treatment. However, how to incorporate the external fields, spatially unbound operators, in density functional theory or hybrid functionals is still a challenge in the current [28].

6.2 In Situ Characterization of Microstructures under the Action of Multi Fields

It is indispensable for studying the evolution mechanism of microstructure of solid metals during electromagnetic treatment to introduce advanced characterization technologies, such as in-situ electron microscopy and synchrotron X-ray. The results obtained from in-situ characterization are in general more convincing than those from the comparison of with and without electromagnetic treatment. However, the existing in-situ characterization is mostly used for thermal loading, stress loading and current loading [146–148]. A great challenge, the interference of external field on electron beam, should be overcome for strong magnetic field in-situ loading.

In recent years, a large number of researchers studied the microstructure evolutions by the characterization at the same position of the specimens before and after electromagnetic treatment. This approximate "in-situ" observation reflects the evolution law of microstructure of materials under the action of electromagnetic field to a certain extent. For instance, Cai et al. [149, 150] studied the dislocations evolution by comparing the Kernel Average Misorientation maps at the same position after pulsed magnetic field treatment. As shown in Figure 16, it could found that the dislocation density of Ti-6Al-4V alloy increases greatly after MT. Wang et al. [151] observed the voids healing of the M50 steel after electropulsing treatment by quasi in-situ scanning electron microscope. Alshits et al. [145] studied quantitatively the motion of dislocations in Al single crystal before and after magnetic field treatment by selective chemical etching.

6.3 Development of High Efficient Nondestructive Evaluation Methods

As is known to all, the products or specimens have to be destroyed for carrying out the performance tests or microscopic characterization mentioned above to evaluate effect of electromagnetic field on the materials. Obviously, it is very unfavorable for the development of a new ET or MT technology or monitoring the stability of products in the production process. Therefore, the developments of high efficient nondestructive testing technologies are helpful to promote the industrialization of ET or MT.

The common nondestructive testing methods such as ultrasonic testing, eddy current testing and laser testing seem to be incapable for evaluating micro nano size defects and phase transformations. Some studies have shown that the electrical conductivity of the material is closely related to the microstructure and properties of the material [152, 153]. Although it has been reported that electromagnetic field treatment can change the electrical conductivity of materials [154], there has been no quantitative relationship between electrical resistance and mechanical properties of materials. The underlying mechanism of this relationship is also unclear.

7 Conclusions

Based on the above analysis and discuss, it can be found that electronic and magnetic field can exert considerable effects on microstructure of solid metal. The conclusions are summarized as follows:

(1) Compared with the traditional heat treatment, ET not only has the Joule heating effect with the characteristics of fast heating and targeting effect, but also has electromigration effect, skin effect, etc. As a result, it can promote phase transformation speed, change transformation temperature, accelerate recrystallization and heal micro-defects of solid metal.

(2) Magnetic field at room temperature can accelerate dislocation depinning resulting from the change the spin state of electrons in the magnetic field. In addation, in the process of heat treatment in the strong magnetic field, the magnetic energy could affect the phase transition temperature, the morphology and volume fraction of phase transition and the formation of texture.

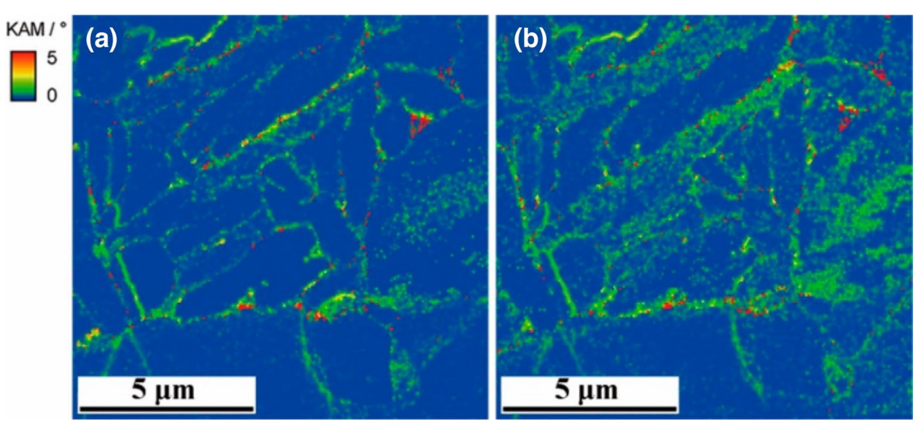

Figure 16 The Kernel Average Misorientation maps of the Ti-6Al-4V specimen (**a**) before MT, (**b**) after MT [149]

(3) The reports of the combination of electronic field and magnetic field treatment are relatively rare so far. Some literatures have shown that its effect is not simply the superposition of separate field treatment, and more desirable results may be achieved due to a wider range of energy density regulation, better adaptability of materials and structures, and so on.
(4) In view of the importance and complexity of the research on the effect of electromagnetic field on microstructure of solid metals, the multidisciplinary joint analyses mainly including materials science, electromagnetism and computational science, and the multi-scale characterizations represented by in-situ testing are the technical challenges and research interests in this field.

Acknowledgements
Not applicable.

Authors' Contributions
YS was in charge of the whole trial and conceived the manuscript; WW and YY wrote the manuscript; LH directed and reviewed the manuscript. All authors read and approved the final manuscript.

Authors' information
Yanli Song, born in 1979, is currently a professor at *School of Automotive Engineering, Wuhan University of Technology, China*. His research interests include high-end equipment lightweight and advanced manufacturing technology.
Wenlin Wu, born in 1985, is currently a PhD candidate at *School of Automotive Engineering, Wuhan University of Technology, China*.
Yongqing Yu, born in 1989, is currently a PhD candidate at *School of Automotive Engineering, Wuhan University of Technology, China*.
Lin Hua, born in 1962, is currently a professor at *School of Automotive Engineering, Wuhan University of Technology, China*. His research interests include modern automobile design and manufacturing, automotive lightweight technology and automotive industry engineering.

Funding
Supported by National Key Research and Development Program of China (Grant No. 2020YFA0714900), National Natural Science Foundation of China (Grant Nos. 51975440, 51975441), the 111 Project (Grant No. B17034), and Innovative Research Team Development Program of Ministry of Education of China (Grant No. IRT17R83).

Availability of Data and Materials
All data generated or analysed during this study are included in this published article.

Declarations

Competing Interests
The authors declare no competing financial interests.

Received: 15 January 2021 Revised: 17 September 2021 Accepted: 19 October 2023
Published online: 24 November 2023

References

[1] F B Guo, B H Zhu, L B Jin, et al. Microstructure and mechanical properties of 7A56 aluminum alloy after solution treatment. *Rare Metals*, 2017, 7: 1-8.
[2] S H Kim, H Kim, N J Kim. Brittle intermetallic compound makes ultrastrong low-density steel with large ductility. *Nature*, 2015, 518(7537): 77-79.
[3] J Liu, C Wei, G Yang, et al. A novel combined electromagnetic treatment on cemented carbides for improved milling and mechanical performances. *Metallurgical and Materials Transactions A*, 2018, 49(10): 4798-4808.
[4] C L Liang, K L Lin. The microstructure and property variations of metals induced by electric current treatment: A review. *Materials Characterization*, 2018, 145: 545-555.
[5] O A Troitskii, V I Likhtman. The anisotropy of the action of electron and γ radiation on the deformation of zinc single crystals in the brittle state. *Soviet Physics Doklady*, 1963, 8: 332-334.
[6] N V Zagoruiko. Effect of an electrostatic field and a pulsed magnetic field on the movements of dislocations in sodium chloride. *Soviet Physics-Crystallography*, 1965, 10: 63-67.
[7] M J Kim, K Lee, K H Oh, et al. Electric current-induced annealing during uniaxial tension of aluminum alloy. *Scripta Materialia*, 2014, 75: 58-61.
[8] H Krishnaswamy, M J Kim, S T Hong, et al. Electroplastic behaviour in an aluminium alloy and dislocation density based modelling. *Materials & Design*, 2017, 124: 131-142.
[9] J H Roh, J J Seo, S T Hong et al. The mechanical behavior of 5052-H32 aluminum alloys under a pulsed electric current. *International Journal of Plasticity*, 2014, 58: 84-99.
[10] V Psyk, D Risch, B L Kinsey, et al. Electromagnetic forming—A review. *Journal of Materials Processing Technology*, 2011, 211(5): 787-829.
[11] A V Pokoev, J V Osinskaya. Manifestation of magnetoplastic effect in some metallic alloys. *Defect & Diffusion Forum*, 2018, 383: 180-184.
[12] M I Molotskii. Theoretical basis for electro- and magnetoplasticity. *Materials Science & Engineering A* (Structural Materials:, Properties, Microstructure and Processing), 2000, 287(2): 248-258.
[13] B E Klamecki. Residual stress reduction by pulsed magnetic treatment. *Journal of Materials Processing Technology*, 2003, 141(3): 385-394.
[14] A L Lu, F Tang, X J Luo, et al. Research on residual-stress reduction by strong pulsed magnetic treatment. *Journal of Materials Processing Technology*, 1998, 74(1-3): 259-262.
[15] S Wu, H Y Zhao, A L Lu, et al. Micromechanism of residual stress reduction by low frequency alternating magnetic field treatment. *Journal of Materials Processing Technology*, 2003, 132(1): 198–202.
[16] Y L Song, L Hua. Mechanism of residual stress reduction in low alloy steel by a low frequency alternating magnetic treatment. *Journal of Materials Science & Technology*, 2012, 28(9): 803-808.
[17] A Babutskyi, A Chrysanthou, C Zhao. Effect of pulsed magnetic field pre-treatment of AISI 52100 steel on the coefficient of sliding friction and wear in pin-on-disk tests. *Friction*, 2014, 2(4): 310-316.
[18] A V Komshina, A S Pomel'nikova, N A Nochovnaya. Improvement of alloy VT23 surface quality with magnetic-pulse treatment. *Metal Science and Heat Treatment*, 2015, 57(5-6): 359-363.
[19] A F Yetim, H Kovacı, M Aslan, et al. The effect of magnetic field on the wear properties of a ferromagnetic steel. *Wear*, 2013, 301(1-2): 636-640.
[20] B T Lü, S R Qiao, X Y Sun. Exploration on repairing fatigue damage of steel specimens with magnetic treatment. *Scripta Materialia*, 1999, 40(7): 767-771.
[21] Y Zhao, H C Fang, X D Fan. Slowing down metal fatigue damage with a magnetic field. *Engineering Fracture Mechanics*, 1993, 46(2): 347-352.
[22] A Çelik, A F Yetim, A Alsaran, et al. Effect of magnetic treatment on fatigue life of AISI 4140 steel. *Materials & Design*, 2005, 26(8): 700-704.
[23] F Heringhaus, H J Schneider-Muntau, G Gottstein. Analytical modeling of the electrical conductivity of metal matrix composites: application to Ag–Cu and Cu–Nb. *Materials Science & Engineering A* (Structural Materials: Properties, Microstructure and Processing), 2003, 347(1-2): 9-20.
[24] S I Hong, M A Hill. Mechanical stability and electrical conductivity of Cu–Ag filamentary microcomposites. *Materials Science & Engineering A*, 1999, 264(1–2): 151-158.
[25] J C Cai, W Wei, X Y Hu, et al. Electrical conductivity models in saturated porous media: A review. *Earth-Science Reviews*, 2017, 171: 419-433.

[26] Y J Wei, Y Q Li, L C Zhu, et al. Evading the strength–ductility trade-off dilemma in steel through gradient hierarchical nanotwins. *Nature Communications*, 2014, 5(1): 1-8.
[27] B B He, B Hu, H W Yen, et al. High dislocation density-induced large ductility in deformed and partitioned steels. *Science*, 2017, 357(6355): 1029-1032.
[28] O Guillon, C Elsässer, O Gutfleisch, et al. Manipulation of matter by electric and magnetic fields: Toward novel synthesis and processing routes of inorganic materials. *Materials Today*, 2018, 21(5): 527-536.
[29] D W Ao, X R Chu, Y Yang, et al. Effect of electropulsing treatment on microstructure and mechanical behavior of Ti-6Al-4V alloy sheet under argon gas protection. *Vacuum*, 2018, 148: 230-238.
[30] B Ma, Y Zhao, J Ma, et al. Formation of local nanocrystalline structure in a boron steel induced by electropulsing. *Journal of Alloys and Compounds*, 2013, 549: 77-81.
[31] L C Xie, H J Guo, Y L Song, et al. Effects of electroshock treatment on microstructure evolution and texture distribution of near-β titanium alloy manufactured by directed energy deposition. *Materials Characterization*, 2020, 161: 1-11.
[32] Y Zhou, W Zhang, B Wang, et al. Grain refinement and formation of ultrafine-grained microstructure in a low-carbon steel under electropulsing. *Journal of Materials Research*, 2011, 17(08): 2105-2111.
[33] Z Zhao, G Wang, H Hou, et al. Influence of high-energy pulse current on the mechanical properties and microstructures of Ti-6Al-4V alloy. *Journal of Materials Engineering and Performance*, 2017, 26(10): 5146-5153.
[34] X Li, S Wang, S Zhao, et al. Effect of pulse current on the tensile deformation of SUS304 stainless steel. *Journal of Materials Engineering and Performance*, 2015, 24(12): 5065-5070.
[35] Y S Zheng, G Y Tang, J Kuang, et al. Effect of electropulse on solid solution treatment of 6061 aluminum alloy. *Journal of Alloys and Compounds,* 2014, 615: 849-853.
[36] X Xu, Y Zhao, X Wang, et al. Effect of rapid solid-solution induced by electropulsing on the microstructure and mechanical properties in 7075 Al alloy. *Materials Science and Engineering: A*, 2016, 654: 278-281.
[37] W L Wu, Y L Song, S R Ning, et al. Microstructure evolution and mechanical properties improvement of Al-Zn-Mg-Cu alloys induced by a novel double electroshocking treatment. *Advanced Engineering Materials*, 2020, 2020(22): 2000106-2000113.
[38] H J Jeong, M J Kim, J W Park, et al. Effect of pulsed electric current on dissolution of Mg17Al12 phases in as-extruded AZ91 magnesium alloy. *Materials Science and Engineering: A*, 2017, 684: 668-676.
[39] Y Jiang, G Tang, L Guan, et al. Effect of electropulsing treatment on solid solution behavior of an aged Mg alloy AZ61 strip. *Journal of Materials Research*, 2011, 23(10): 2685-2691.
[40] Y Liu, M Huang, Z Ma, et al. Influence of the low-density pulse current on the ageing behavior of AA2219 aluminum alloy. *Journal of Alloys and Compounds,* 2016, 673: 358-363.
[41] Y T Wang, Y G Zhao, X F Xu, et al. Superior mechanical properties induced by the interaction between dislocations and precipitates in the electro-pulsing treated Al-Mg-Si alloys. *Materials Science and Engineering: A*, 2018, 735: 154-161.
[42] J E Garay, U Anselmi-Tamburini, Z A Munir. Enhanced growth of intermetallic phases in the Ni–Ti system by current effects. *Acta Materialia*, 2003, 51(15): 4487-4495.
[43] G Peng, K Chen, S Chen, et al. Evolution of the second phase particles during the heating-up process of solution treatment of Al–Zn–Mg–Cu alloy. *Materials Science and Engineering: A*, 2015, 641: 237-241.
[44] Y C Xing, Q A Lv, Z Y Li, et al. Analysis and simulation on pulse current distribution in copper strips. *2014 17th International Symposium on Electromagnetic Launch Technology (EML), IEEE*, 2014.
[45] Y Dolinsky, T Elperin. Thermodynamics of phase transitions in current-carrying conductors. *Physical Review B*, 1993, 47(22): 14778-14785.
[46] Y Dolinsky, T Elperin. Thermodynamics of nucleation in current-carrying conductors. *Physical Review B*, 1994, 50(1): 52-58.
[47] R Qin, H Yan, H E Guang, et al. Exploration on the fabrication of bulk nanocrystalline materials by direct-nanocrystallizing method-I theoretical calculation of grain size of metals sondified under electropulsing. *Chinese Journal of Material Research*, 1995, 9(3): 219-222.
[48] H Song, Z Wang. Grain refinement by means of phase transformation and recrystallization induced by electropulsing. *Transactions of Nonferrous Metals Society of China*, 2011, 21: s353-s357.
[49] X Xu, Y Zhao, B Ma, et al. Rapid grain refinement of 2024 Al alloy through recrystallization induced by electropulsing. *Materials Science and Engineering: A*, 2014, 612(26): 223-226.
[50] Y Liu, J Fan, H Zhang, et al. Recrystallization and microstructure evolution of the rolled Mg–3Al–1Zn alloy strips under electropulsing treatment. *Journal of Alloys and Compounds*, 2015, 622: 229-235.
[51] H Conrad. Effects of electric current on solid state phase transformations in metals. *Materials Science & Engineering: A*, 2000, 287(2): 227-237.
[52] H Conrad, Z Guo, A F Sprecher. Effect of an electric field on the recovery and recrystallization of Al and Cu. *Scripta Metallurgica*, 1989, 23(6): 821-823.
[53] A L Hu, G Y Tang, L Guan, et al. Difference in recrystallization between electropulsing-treated and furnace-treated NiTi alloy. *Journal of Alloys and Compounds: An Interdisciplinary Journal of Materials Science and Solid-state Chemistry and Physics*, 2016, 658: 548-554.
[54] S Liu, J Zhu, X D Lin, et al. Coupling effect of stretch-bending deformation and electric pulse treatment on phase transformation behavior and superelasticity of a Ti-50.8at.% Ni alloy. *Materials Science & Engineering A*, 2021, 799: 140164 (1-10).
[55] S Lin, X Chu, Z Yue, et al. Effect of temperature on the dynamic recrystallization of AZ31 alloy with pulse current. *Acta Metallurgica Sinica*, 2018, 31(12): 53-58.
[56] G Hu, C Shek., Y Zhu, et al. Effect of electropulsing on recrystallization of Fe-3%Si alloy strip. *Materials Transactions*, 2010, 51(8): 1390-1394.
[57] H Conrad, N Karam, S Mannan. Effect of prior cold work on the influence of electric current pulses on the recrystallization of copper. *Scripta Metallurgica*, 1984, 18(3): 275–280.
[58] S Xiang, X Zhang. Dislocation structure evolution under electroplastic effect. *Materials Science & Engineering A*, 2019, 761(JUL.22): 138026.138021-138026.
[59] J Zhu, S Liu, Y Lin, et al. Effect of electropulsing on microstructure and properties of severely plastically deformed pure copper sheet. *Journal of Materials Engineering and Performance,* 2020, 29(2): 841-848.
[60] S Zhao, R Zhang, Y Chong, et al. Defect reconfiguration in a Ti-Al alloy via electroplasticity. *Nature Materials*, 2020, https://doi.org/10.1038/s41563-020-00817-z
[61] L B Zuev, V E Gromov, V F Kurilov, et al. Mobility of dislocations in zinc single crystals under the action of electric current pulses. *Soviet Phys. Dokl*, 1978, 23: 199-200.
[62] M I Molotskii. Theoretical basis for electro- and magnetoplasticity. *Materials Science and Engineering A*, 2000, 287(2): 248-258.
[63] V I Dubinko, V F Klepikov. Kinetic mechanism of the electroplastic effect in metals. *Bulletin of the Russian Academy of Sciences. Physics,* 2008, 72(9): 1188-1189.
[64] D W Tang, B L Zhou, H Cao, et al. Thermal stress relaxation behavior in thin films under transient laser pulse heating. *Journal of Applied Physics*, 1993, 73(8): 3749-3752.
[65] C L Yang, H J Yang, Z J Zhang, et al. Recovery of tensile properties of twinning-induced plasticity steel via electropulsing induced void healing. *Scripta Materialia*, 2018, 147: 88-92.
[66] A Hosoi, T Nagahama, Y Ju. Fatigue crack healing by a controlled high density electric current field. *Materials Science and Engineering: A*, 2012, 533: 38-42.
[67] J Jung, Y Ju, Y Morita, et al. Enhancement of fatigue life of aluminum alloy affected by the density of pulsed electric current. *International Journal of Fatigue*, 2017, 103: 419-425.
[68] H Song, Z J Wang. Microcrack healing and local recrystallization in predeformed sheet by high density electropulsing. *Materials Science and Engineering: A*, 2008, 490(1-2): 1-6.
[69] H Conrad, J White, W D Cao, et al. Effect of electric current pulses on fatigue characteristics of polycrystalline copper. *Materials Science & Engineering A*, 1991, 145(1): 1-12.
[70] R Qin, S Su. Thermodynamics of crack healing under electropulsing. *Journal of Materials Research*, 2002, 17(08): 2048-2052.
[71] G R Li, Y M Li, F F Wang, et al. Microstructure and performance of solid TC4 titanium alloy subjected to the high pulsed magnetic field treatment. *Journal of Alloys and Compounds*, 2015, 644: 750-756.
[72] J Li, W Liu. Effects of high magnetic field on isothermal pearlite transformation and microstructure in a hypereutectoid steel. *Journal of Magnetism and Magnetic Materials,* 2014, 362: 159-164.

[73] M Miglierini, V Procházka, R Rüffer, et al. In situ crystallization of metallic glasses during magnetic field annealing. *Acta Materialia*, 2015, 91: 50-56.
[74] S Rivoirard. High steady magnetic field processing of functional magnetic materials. *JOM*, 2013, 65(7): 901-909.
[75] T Garcin, S Rivoirard, C Elgoyhen, et al. Experimental evidence and thermodynamics analysis of high magnetic field effects on the austenite to ferrite transformation temperature in Fe–C–Mn alloys. *Acta Materialia*, 2010, 58(6): 2026-2032.
[76] K R Satyanarayan, W Eliasz, A P Miodownik. The effect of a magnetic field on the martensite transformation in steels. *Acta Metallurgica*, 1968, 16(6): 877-887.
[77] H D Joo, S U Kim, Y M Koo, et al. An effect of a strong magnetic field on the phase transformation in plain carbon steels. *Metallurgical and Materials Transactions A*, 2004, 35(6): 1663-1668.
[78] J Liu, T Gottschall, K P Skokov, et al. Giant magnetocaloric effect driven by structural transitions. *Nature Materials*, 2012, 11(7): 620-626.
[79] N M Bruno, S Wang, I Karaman, et al. Reversible martensitic transformation under low magnetic fields in magnetic shape memory alloys. *Scientific Reports*, 2017, 7(1): 1-10.
[80] J Y Choi, T Fukuda, T Kakeshita. Effect of magnetic field on isothermal martensitic transformation in a sensitized SUS304 austenitic stainless steel. *Journal of Alloys and Compounds*, 2013, 577: S605-S608.
[81] T Fukuda, T Kakeshita. Advanced materials design by controlling transformation temperature using magnetic field. *Springer Japan*, 2013, https://doi.org/10.1007/978-4-431-54064-9_14169-180.
[82] T Kakeshita, T Saburi, K Kind, et al. Martensitic transformations in some ferrous and non-ferrous alloys under magnetic field and hydrostatic pressure. *Phase Transitions*, 1999, 70(2): 65-113.
[83] M Enomoto, H Guo, Y Tazuke, et al. Influence of magnetic field on the kinetics of proeutectoid ferrite transformation in iron alloys. *Metallurgical & Materials Transactions A*, 2001, 32(3): 445-453.
[84] X J Hao, H Ohtsuka, H Wada. Structural elongation and alignment in an Fe-0.4C alloy by isothermal ferrite transformation in high magnetic fields. *Materials Transactions*, 2003, 44(12): 2532-2536.
[85] M Shimotomai, K Maruta, K Mine, et al. Formation of aligned two-phase microstructures by applying a magnetic field during the austenite to ferrite transformation in steels. *Acta Materialia*, 2003, 51(10): 2921-2932.
[86] Y Zhang, N Gey, C He, et al. High temperature tempering behaviors in a structural steel under high magnetic field. *Acta Materialia*, 2004, 52(12): 3467-3474.
[87] H M Wang, G Li, Y M Li, et al. Influence of high magnetic field on β-a phase transformation in TC4 titanium alloy. *Advanced Materials Research*, 2014, 941-944: 112-115.
[88] X Zuo, C Zhao, R Niu, et al. Microstructural dependence of magnetoresistance in CuAg alloy solidified with high magnetic field. *Journal of Materials Processing Technology*, 2015, 224: 208-212.
[89] P Lázpita, M Sasmaz, E Cesari, et al. Martensitic transformation and magnetic field induced effects in Ni 42 Co 8 Mn 39 Sn 11 metamagnetic shape memory alloy. *Acta Materialia*, 2016, 109: 170-176.
[90] M L Gong, F F Liu, X Zhao, et al. Effects of a high magnetic field on abnormal microstructure in Fe-1.1C (wt.%) alloy. *Advanced Materials Research*, 2012, 496: 467-471.
[91] Y Yuan, Q Wang, K Iwai, et al. Isothermal heat treatments of an Al–4.8mass%Cu alloy under high magnetic fields. *Journal of Alloys and Compounds*, 2013, 560: 127-131.
[92] H Ohtsuka. Effects of strong magnetic fields on bainitic transformation. *Current Opinion in Solid State and Materials Science*, 2004, 8(3-4): 279-284.
[93] L He, X Li, P Zhu, et al. Effects of high magnetic field on the evolutions of constituent phases in 7085 aluminum alloy during homogenization. *Materials Characterization*, 2012, 71: 19-23.
[94] J K Choi, H Ohtsuka, Y Xu, et al. Effects of a strong magnetic field on the phase stability of plain carbon steels. *Scripta Materialia*, 2000, 43(3): 221-226.
[95] X Y Sun, C L Chen, L Yang, et al. Experimental study on modulated structure in Alnico alloys under high magnetic field and comparison with phase-field simulation. *Journal of Magnetism and Magnetic Materials*, 2013, 348: 27-32.
[96] F Gaucherand, E Beaugnon. Magnetic texturing in ferromagnetic cobalt alloys. *Physica B: Condensed Matter*, 2004, 346-347: 262-266.
[97] H Ohtsuka. Structural control of Fe-based alloys through diffusional solid/solid phase transformations in a high magnetic field. *Science and Technology of Advanced Materials*, 2008, 9(1): 13004-13004.
[98] J Y Song, Y D Zhang, X Zhao, et al. Effects of high magnetic field strength and direction on pearlite formation in Fe–0.12%C steel. *Journal of Materials Science*, 2008, 43(18): 6105-6108.
[99] Y D Zhang, C Esling, J S Lecomte, et al. Grain boundary characteristics and texture formation in a medium carbon steel during its austenitic decomposition in a high magnetic field. *Acta Materialia*, 2005, 53(19): 5213-5221.
[100] Y Zhang, C He, X Zhao, et al. New microstructural features occurring during transformation from austenite to ferrite under the kinetic influence of magnetic field in a medium carbon steel. *Journal of Magnetism and Magnetic Materials*, 2004, 284: 287-293.
[101] Z Sun, M Guo, J Vleugels, et al. Strong static magnetic field processing of metallic materials: A review. *Current Opinion in Solid State and Materials Science*, 2012, 16(5): 254-267.
[102] K Kang, L H Lewis, A R Moodenbaugh. Alignment and analyses of MnBi/Bi nanostructures. *Applied Physics Letters*, 2005, 87(6): 6053.
[103] S Asai, K S Sassa, M Tahashi. Crystal orientation of non-magnetic materials by imposition of a high magnetic field. *Science and Technology of Advanced Materials*, 2003, 4(5): 455-460.
[104] T Zheng, Y Zhong, Z Lei, et al. Effects of high static magnetic field on crystal orientation and magnetic property of Bi-5wt.% Zn alloys. *Materials Letters*, 2015, 140: 68-70.
[105] X Feng, K Kawabata, M G Cowan, et al. Single crystal texture by directed molecular self-assembly along dual axes. *Nature Materials*, 2019, 18: 1235–1243.
[106] Z Sun, M Guo, J Vleugels, et al. Strong magnetic field-induced segregation and alignment of nonmagnetic particles. *Journal of Applied Physics*, 2011, 109(7): 277.
[107] C Wang, Q Wang, Z Wang, et al. Phase alignment and crystal orientation of Al3Ni in Al–Ni alloy by imposition of a uniform high magnetic field. *Journal of Crystal Growth*, 2008, 310(6): 1256-1263.
[108] A E Mikelson, Y K Karklin. Control of crystallization processes by means of magnetic fields. *Journal of Crystal Growth*, 1981, 52(4): 524-529.
[109] W W Mullins. Magnetically induced grain-boundary motion in bismuth. *Acta Metallurgica*, 1956, 4(4): 421-432.
[110] D A Molodov, N Bozzolo. Observations on the effect of a magnetic field on the annealing texture and microstructure evolution in zirconium. *Acta Materialia*, 2010, 58(10): 3568-3581.
[111] D A Molodov, A D Sheikh-Ali. Effect of magnetic field on texture evolution in titanium. *Acta Materialia*, 2004, 52(14): 4377-4383.
[112] V I Alshits, E V Darinskaya, O L Kazakova, et al. Magnetoplastic effect in non-magnetic crystals and internal friction. *Journal of Alloys & Compounds*, 1994, 211(212): 548-553.
[113] V I Alshits, E V Darinskaya, M V Koldaeva, et al. Dislocation kinetics in nonmagnetic crystals: a look through a magnetic window. *Physics Uspekhi*, 2017, 60(3): 305-318.
[114] Y I Golovin, R B Morgunov, V E Ivanov. In situ investigation of the effect of a magnetic field on the mobility of dislocations in deformed KCl:Ca single crystals. *Physics of The Solid State*, 1997, 39(4): 550-553.
[115] M V Koldaeva, V I Alshits, E A Petrzhik, et al. Low-frequency spectra of dislocation paths in NaCl crystals in the electron spin resonance scheme. *Bulletin of the Russian Academy of ences Physics*, 2014, 78(10): 1086-1091.
[116] G Tang, Z Xu, M Tang, et al. Effect of a pulsed magnetic treatment on the dislocation substructure of a commercial high strength steel. *Materials Science and Engineering: A*, 2005, 398(1-2): 108-112.
[117] L Ma, W Zhao, Z Liang, et al. An investigation on the mechanical property changing mechanism of high speed steel by pulsed magnetic treatment. *Materials Science and Engineering: A*, 2014, 609: 16-25.
[118] C Yu. Control process and mechanism of magnetic treatment on microstructures, properties and residual stress of auto tailor welded blanks. Wuhan: Wuhan University of Technology, 2017. (in Chinese)

[119] Y L Song, C Yu, H Yu, et al. Mechanical properties improvement of laser tailor welded blanks of DP600 steel by magnetic treatment. *Metals*, 2017, 7(3): 85-91.
[120] P J Ferreira, J Sande. Magnetic field effects on twin dislocations. *Scripta Materialia*, 1999, 41(2): 117-123.
[121] Y I Golovin. Mechanochemical reactions between structural defects in magnetic fields. *Journal of Materials Science*, 2004, 39(16-17): 5129-5134.
[122] S N Prasad, P N Singh, V Singh. Influence of pulsating magnetic field on softening behaviour of cold rolled AISI 4340 steel at room temperature. *Scripta Materialia*, 1996, 34(12): 1857-1860.
[123] G R Li, F F Wang, H M Wang, et al. Microstructure and mechanical properties of TC4 titanium alloy subjected to high static magnetic field. *Materials Science Forum*, 2017, 898: 345-354.
[124] J F Cheng, G R Li, H M Wang, et al. Influence of high pulsed magnetic field on the dislocations and mechanical properties of Al2O3/Al composites. *Journal of Materials Engineering and Performance*, 2018, 27(3): 1083-1092.
[125] S Wu, H Y Zhao, A Lu, et al. Micro-mechanism model of residual stress relaxation in steels by magnetic treatment. *Journal of Tsinghua University*, 2002, 42(2): 147-150. (in Chinese)
[126] C Li, S He, H Engelhardt, et al. Alternating-magnetic-field induced enhancement of diffusivity in Ni-Cr alloys. *Scientific Reports*, 2017, 7(1): 18085.
[127] X Hu, L Peng, S Qian, et al. Effects of intermediate frequency magnetic field on the solution treatment of Mg–Gd alloy. *Materials Letters*, 2014, 123: 238-241.
[128] R Chen, C Wang, P Jiang, et al. Effect of axial magnetic field in the laser beam welding of stainless steel to aluminum alloy. *Materials & Design*, 2016, 109: 146-152.
[129] Z Cai, X Huang. Residual stress reduction by combined treatment of pulsed magnetic field and pulsed current. *Materials Science and Engineering: A*, 2011, 528(19-20): 6287-6292.
[130] A I Pinchook, S D Shavrey. Effect of a constant magnetic field and a pulse electric current on the mean linear density of twinning dislocations in bismuth crystals. *Physics of The Solid State*, 2001, 43(8): 1476-1477.
[131] A I Pinchook, S D Shavrey. A correlation between the microhardness and the mobility of twinning dislocations in bismuth crystals exposed to constant magnetic field and pulsed electric field. *Technical Physics Letters*, 2002, 28(6): 525-526.
[132] X J Rao, Y B Zhong, Z G Zhang, et al. Electrical and mechanical properties of a Cu-Cr-Zr alloy aged under an imposed DC current and static magnetic field. *Acta Physica Sinica*, 2012, 61(22): 173-181. (in Chinese)
[133] Z P Lai, Q L Cao, B Zhang, et al. Radial Lorentz force augmented deep drawing for large drawing ratio using a novel dual-coil electromagnetic forming system. *Journal of Materials Processing Technology*, 2015, 222: 13–20.
[134] Z Cao, Y Zuo. Electromagnetic riveting technique and its applications. *Chinese Journal of Aeronautics*, 2020, 33(1): 5-15.
[135] J Shang, G Daehn. Electromagnetically assisted sheet metal stamping. *Journal of Materials Processing Tech.*, 2015, 211(5): 868-874.
[136] J J Jones, L Mears, J T Roth. Electrically-assisted forming of magnesium AZ31: Effect of current magnitude and deformation rate on forgeability. *Journal of Manufacturing Science and Engineering*, 2012, 134(3): 034501-034507.
[137] R Zhu, G Tang, S Shi, et al. Effect of electroplastic rolling on deformability and oxidation of NiTiNb shape memory alloy. *Journal of Materials Processing Technology*, 2013, 213(1): 30-35.
[138] E Sánchez, J Antonio, R González, et al. Mechanical and metallurgical changes on 308L wires drawn by electropulses. *Materials & Design*, 2016, 90(JAN): 1159-1169.
[139] Y Zhao, L Peng, X Lai. Influence of the electric pulse on springback during stretch U-bending of Ti6Al4V titanium alloy sheets. *Journal of Materials Processing Technology*, 2018, 261: 12-23.
[140] H Saqib, G R Hernán, P B José, et al. Influence of the regime of electropulsing-assisted machining on the plastic deformation of the layer being cut. *Materials*, 2018, 11(886): 1-10.
[141] W L Wu, Y L Song, Z Q Wang, et al. Solid phase transformation of Ti–6.6Al–3.4Mo alloy induced by electroshocking treatment. *Journal of Materials Science*, 2019, 2019(1): 1-11.
[142] X D Song, F Wang, D Qian, et al. Tailoring the residual stress and mechanical properties by electroshocking treatment in cold rolled M50 steel. *Materials Science and Engineering: A*, 2020, 780: 139171-139179.
[143] L C Xie, C Liu, Y L Song, et al. Evaluation of microstructure variation of TC11 alloy after electroshocking treatment. *Journal of Materials Research and Technology*, 2020, 9(2): 2455-2466.
[144] P D Goldman, L R Motowidlo, J M Galligan. The absence of an electroplastic effect in lead at 4.2K. *Scripta Metallurgica*, 1981, 15: 353-356.
[145] V I Al'shits, E V Darinskaya, E Y Mikhina, et al. On the nature of the influence of an electric current on the magnetically stimulated microplasticity of Al single crystals. *Journal of Experimental & Theoretical Physics Letters*, 1998, 67(10): 832-838.
[146] Z Kou, Y Yang, L Yang, et al. Dynamic interactions between non-screw dislocations and stacking faults during in situ straining in a TEM. *Materials Characterization*, 2019, 148: 292-296.
[147] Z Kou, Y Yang, L Yang, et al. New role of screw dislocation in twin lamella during deformation: An in situ TEM study at the atomic scale. *Materials Science and Engineering: A*, 2018, 729: 125-129.
[148] X Li, A M Minor. In situ TEM investigation of the electroplasticity phenomenon in metals. *Microscopy and Microanalysis*, 2019, 25(S2): 1832-1833.
[149] X Zhang, Q Zhao, Z Cai, et al. Effects of magnetic field on the residual stress and structural defects of Ti-6Al-4V. *Metals*, 2020, 10(1): 141-148.
[150] M Hou, K Li, X Li, et al. Effects of pulsed magnetic fields of different intensities on dislocation density, residual stress, and hardness of Cr4Mo4V steel. *Crystals*, 2020, 10(2): 115-123.
[151] F Wang, D Qian, L Hua, et al. Voids healing and carbide refinement of cold rolled M50 bearing steel by electropulsing treatment. *Scientific Reports*, 2019, 9(1): 11315.
[152] Y Liu, D M Jiang, W J Li. The effect of multistage ageing on microstructure and mechanical properties of 7050 alloy. *Journal of Alloys and Compounds*, 2016, 671: 408-418.
[153] A F Oliveira, M C de Barros, K R Cardoso, et al. The effect of RRA on the strength and SCC resistance on AA7050 and AA7150 aluminium alloys. *Materials Science and Engineering: A*, 2004, 379(1-2): 321-326.
[154] Z Lin, H Ke, W Engang, et al. Effect of 31.2T magnetic field on microstructure and performance of an Ag-45.8wt%Ni alloy. *Journal of Iron & Steel Research*, 2012, S2: 1063-1067.

Submit your manuscript to a SpringerOpen journal and benefit from:

- ► Convenient online submission
- ► Rigorous peer review
- ► Open access: articles freely available online
- ► High visibility within the field
- ► Retaining the copyright to your article

Submit your next manuscript at ► springeropen.com